Evaluation of the forecasting model for current, wave and wind at DanWEC

Têtu, Amélie

Publication date:
2018

Document Version
Publisher's PDF, also known as Version of record

DEPARTMENT OF CIVIL ENGINEERING
AALBORG UNIVERSITY

Evaluation of the forecasting model for current, wave and wind at DanWEC

Amélie Têtu

ISSN 1901-726X

DCE Technical Report No. 224

Aalborg University
Department of Civil Engineering
Group Name

DCE Technical Report No. 224

Evaluation of the forecasting model for current, wave and wind at DanWEC

December 2018

Scientific Publications at the Department of Civil Engineering

Technical Reports are published for timely dissemination of research results and scientific work carried out at the Department of Civil Engineering (DCE) at Aalborg University. This medium allows publication of more detailed explanations and results than typically allowed in scientific journals.

Technical Memoranda are produced to enable the preliminary dissemination of scientific work by the personnel of the DCE where such release is deemed to be appropriate. Documents of this kind may be incomplete or temporary versions of papers—or part of continuing work. This should be kept in mind when references are given to publications of this kind.

Contract Reports are produced to report scientific work carried out under contract. Publications of this kind contain confidential matter and are reserved for the sponsors and the DCE. Therefore, Contract Reports are generally not available for public circulation.

Lecture Notes contain material produced by the lecturers at the DCE for educational purposes. This may be scientific notes, lecture books, example problems or manuals for laboratory work, or computer programs developed at the DCE.

Theses are monograms or collections of papers published to report the scientific work carried out at the DCE to obtain a degree as either PhD or Doctor of Technology. The thesis is publicly available after the defence of the degree.

Latest News is published to enable rapid communication of information about scientific work carried out at the DCE. This includes the status of research projects, developments in the laboratories, information about collaborative work and recent research results.

Published 2018 by

Aalborg University

Department of Civil Engineering

Thomas Manns Vej 23

DK-9220 Aalborg Ø, Denmark

Printed in Aalborg at Aalborg University

ISSN 1901-726X

DCE Technical Report No. 224

Introduction

In the process of setting up the Danish test site for wave energy Aalborg University and DHI have collaborated with DanWEC [1] to provide dedicated descriptions of the wave climate at the site by hindcast wave modelling and setting up a forecast system. The detailed assessment of the wave climate both in terms of wave energy resource and extreme conditions are imperative for developers in order to be able to accurately design the wave energy converters (WECs) to the test site. The characterization of the wave climate was done based on 35 years hindcast modelling applying DHI's model MIKE 21 SW [2] and is available in [3]. The dedicated MIKE 21 wave model was also applied as the basis for setting up a forecast service. The forecast updates a range of parameters related to the wave conditions, wind conditions and current speed throughout the modelling area twice every 24 hours [4]. The forecast model provide a 5 days prognostic of the conditions at the test site and the model forcing comprises input from regional DHI models and wind fields.

The forecast is a valuable tool to plan operations at the test site. An O&M decision support system is being build as assistance to the operators.

This report will first give an introduction to the test site and its sensor network. The hindcast model which is used as base for the forecast model will be introduced together with validation of the model against data from wave measuring buoys. The forecast system and the ability of the forecast to accurately predict the wave and current conditions will then be presented. A detail analysis of the accuracy of the forecast model is presented using different error metrics and analyzing the data on a seasonal and monthly basis.

2. Description of the DanWEC test site

The DanWEC test site is situated on the North-West coast of the Danish peninsula Jutland, at Hanstholm, facing the Danish part of the North Sea. The data acquisition network of the test site comprises three buoys, as shown in Fig. 1. It consists of one Datawell Mark II non directional buoy, placed outside Hantsholm's harbour, and two Datawell DWR4 directional buoys including current measurements. The non-directional buoy “Buoy I” has been installed in 1998 and has provided almost 20 years of data [5]. Before 1998 a similar older version of a wave rider buoy was placed outside the harbour and paper records of wave data over the period 1979 1988 was analysed in relation to the first Wave Power experiments by Danish Wave Power Aps in 1989 [5].

Table 1. DanWEC wave measurement instrumentation

	Coordinates (Lat [°], Lon [°])	Water depth [m]	Model
Buoy I	(57.1315, 8.5821)	17.5	Datawell Mark II non directional
Buoy II	(57.1112, 8.5457)	14.5	Datawell DRW4 directional wave and current
Buoy III	(57.1171, 8.5173)	24.6	Datawell DRW4 directional wave and current

The two DanWEC directional buoys were installed in March 2015 and have been providing new information on the wave climate at this location, including insight on the directionality of the waves, the wave spectra and current characteristics. The two directional buoys are situated at a distance of approximately 3 km from the shore and are equipped with accelerometers providing displacements over time after proper filtering and double integration. The accelerometer measuring

the vertical displacement is placed on a gravity-stabilized platform, decoupling the movement of the buoy from the measurement of the wave height through vertical acceleration. The directional buoys are also equipped with three acoustic current transducers placed 120° laterally apart. They measure the Doppler shift of reflected 2 MHz pings at roughly 1 m water depth. All directions are measured relative to the north magnetic pole as both systems are equipped with a magnetic compass. The directional buoys measure the north, west and vertical displacements at a rate of 2.56 Hz and the raw data is transferred to a computer onshore through a radio link signal. The current measurement is taken every 10 minutes and is sent by radio link signal to the same computer onshore. The raw data is processed with Datawell Waves4 software suite [6]. Fourier analysis is used to obtain the spectral parameters from the horizontal and vertical displacements over a period of 30 minutes. Frequency-domain parameters are available for Buoy I, II, and III. Table 2 lists the parameters provided by Buoy I, while Tab. 3 lists the parameters for Buoy II and III. The water depth in the test site varies from 15 meter closest to the coast to about 25 meter at the deepest. In general the seabed is covered with sand and silt, however at some locations this cover is washed away and the chalk is exposed. DanWEC has carried out a geotechnical survey of the test area which defines the water depth variation as well as the typical variation of the sediments. This information is made available for developers that enter a testing agreement with DanWEC.

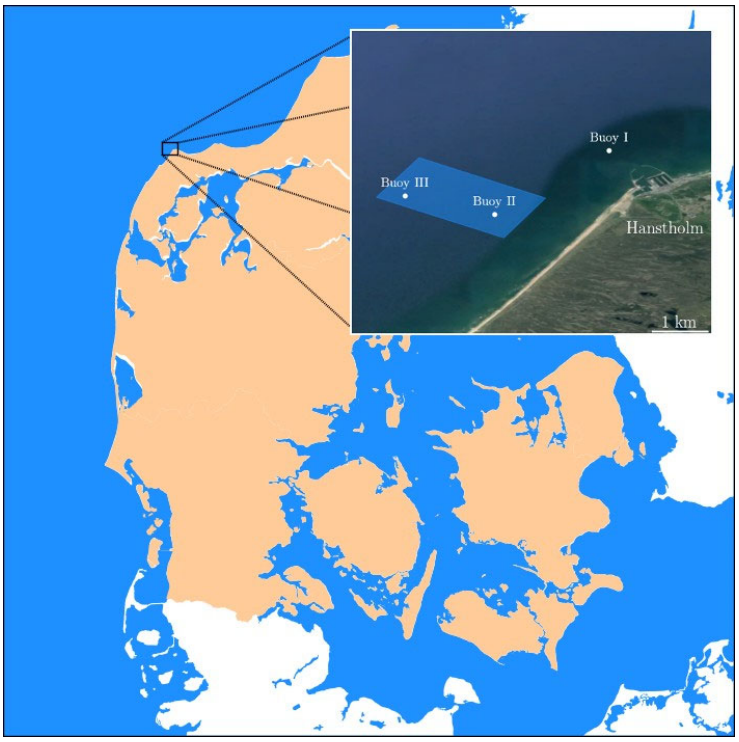

Fig. 1. DanWEC network sensor situated on the north-west coast of mainland Denmark.

Wind data is also available for the location. It is measured using an anemometer located at the Port of Hanstholm. The data is continuously transmitted to www.hyde.dk. The data presented in table 4 from the website is added to the DanWEC database.

Table 2. Frequency-domain parameters for Buoy I

Symbol	Unit	Title
H_{m0}	[m]	Significant wave height
T_e	[s]	Energy wave period
$T_{0,1}$	[s]	Mean wave period
T_z	[s]	Zero-crossing wave period
T_p	[s]	Peak wave period
ϵ	[-]	Spectral bandwidth
L_p	[m]	Peak wavelength
P_w	[W/m]	Wave power

Table 3. Frequency-domain parameters for Buoy II and III

Symbol	Unit	Title
H_{m0}	[m]	Significant wave height
T_e	[s]	Energy wave period
$T_{0,1}$	[s]	Mean wave period
T_z	[s]	Zero-crossing wave period
T_c	[s]	Crest wave period
T_p	[s]	Peak wave period
Θp	[-]	Mean wave direction
σ_p	[rad]	Spread of the mean direction
P_w	[W/m]	Wave power

Table 4. Weather data included in the DanWEC database

Parameter	Unit
End sample time (UTC)	[-]
Water level	[m]
Mean wind speed	[m/s]
Wind direction	[°]
Wind gust	[m/s]
Pressure	[bar]
Temperature	[°C]

3. Wave and current climate model for DanWEC

The forecast model for the DanWEC test site has been based on the hindcast model for the area. The later will be introduced together with its validation against data from wave measuring buoys. The forecast model will afterwards be presented.

3.1. Hindcast model

The forecast model is based on a hindcast model of the DanWEC test site. For the hindcast model the numerical model used is the MIKE 21 Spectral Wave (SW) model version 2016 [7]. MIKE 21 SW includes the following physical phenomena:

- Wave growth by action of wind
- Non-linear wave-wave interaction (quadruplet and triad-wave interactions)
- Dissipation due to white-capping
- Dissipation due to bottom-friction
- Dissipation due to depth-induced wave breaking
- Refraction and shoaling (due to depth variations and currents)
- Wave-current interaction
- Effect of time-varying water depth and currents

Wave diffraction and wave reflection are not included in this study as no island, headland or other obstruction are present in the area under study. The effect of ice coverage on the wave field is also not relevant for the area under study. The frequency discretization was 25 bins with a minimum frequency of 0.033 Hz and a logarithmic frequency increment factor of 1.15 resulting in resolved wave periods in the interval [1.2, 33.3] s ([0.033, 0.945] Hz).

The output wave data covers the period from January 15, 1981 to December 31, 2015, a total of 35 years. The number of azimuthal directions in the numerical model is 24. A maximum (adaptive) computational time step of 300 s was applied and the output time step is 1 hour. The bathymetry and grid resolution used in the numerical model are presented in Fig. 2.

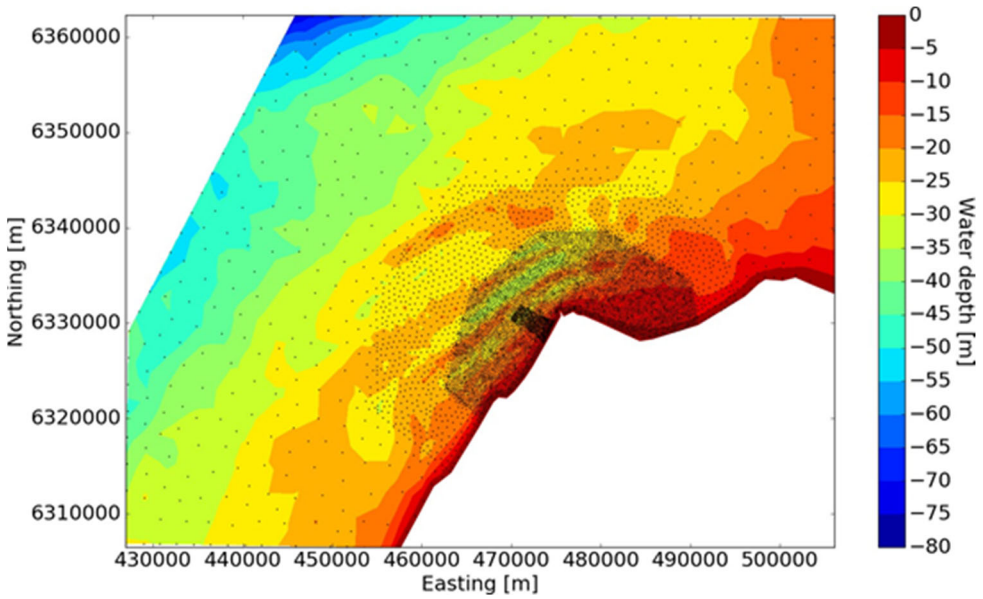

Fig. 2. Bathymetry and mesh resolution used in MIKE 21 Spectral Wave model to obtain the 35 years hindcast data at the DanWEC test site.

Wind forcing was applied with an uncoupled air-sea interaction process. The wind energy momentum transfer to the water was calibrated through the Charnock parameter, which directly influences the amount of energy transferred from the wind to the build-up waves. A Charnock parameter of 0.0185 was applied, which is commonly used for coastal areas. A cap was introduced for the ratio of friction velocity to wind speed ($U/U10$) [8]. The cap was

set at 0.055 [8]. This cap limits the momentum transfer and is based on the documented concept of a saturation of the drag coefficient at extreme storm wind speeds.

Depth-induced wave breaking is a process by which waves dissipate energy when the waves are too high to be stable at the local water depth, i.e. exceeding a limiting wave height to depth ratio. The breaking parameter, γ, varies significantly depending on the wave conditions and the bathymetry. The γ parameter controlling the limiting water depth and the α parameter controlling the rate of dissipation were applied with the default (average) values of $\gamma = 0.8$ and $\alpha = 1$ (see [9, 10]).

Bottom friction was described through the Nikuradse roughness, meaning that the bottom friction varies with the orbital characteristics of the wave close to the bottom. The applied roughness was $k_N = 0.04$ m.

For the boundary conditions, spectral wave data from the Spectral Wave model Northern Europe (SWNE) is applied along the open boundaries. The SW_{NE} was validated with data from two different stations: Fjaltring NE and Hirtshals West. This model takes into account coastal reflections. More information is available in [11].

White-capping, a process by which waves dissipate energy, is primarily controlled by the steepness of the waves. The C_{dis} coefficient is a proportional factor on the white-capping dissipation source function and thus controls the overall dissipation rate. The $DELTA_{dis}$ coefficient controls the weight of dissipation in the energy/action. These parameters were found from calibration, and are within the range of typically adopted parameters in coastal applications.

3.2. Hindcast model validation

The model was validated against wave measurements from Buoy I, Buoy II and Buoy III. Scatter plots of modelled and observed data is presented in [11]. As an example, a very good agreement between measured and modelled data is shown in Fig. 3 where a snap shot in time between the 12th of September 2015 and the 9th of October 2015 is taken. The results of the validation are summarized in Tab. 5, 6 and 7. The quality indices are defined in terms of the observed data (X), the modelled data (Y), and the number of synchronized data used for the validation (N).

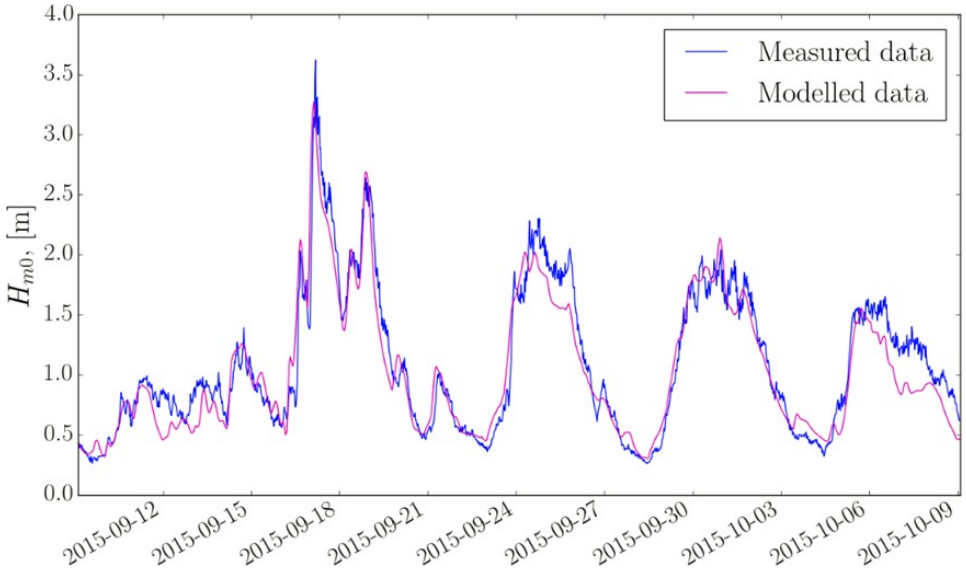

Fig. 3. Measured and modelled data between the 12th of September 2015 and the 9th of October 2015 at the reference point.

$\overline{Y}$ stands for the average of the modelled data Y:

$$\bar{Y} = \frac{1}{N}\sum_{i=1}^{N} Y_i$$

$\overline{X}$ stands for the average of the observed data X:

$$\bar{X} = \frac{1}{N}\sum_{i=1}^{N} X_i$$

$BIAS$ is the mean difference:

$$BIAS = \frac{1}{N}\sum_{i=1}^{N} (Y - X)_i$$

AME is the absolute mean difference:

$$AME = \frac{1}{N}\sum_{i=1}^{N} (|Y - X|)_i$$

$RMSE$ is the root mean square difference:

$$RMSE = \sqrt{\frac{1}{N}\sum_{i=1}^{N} (Y - X)_i^2}$$

SI is the scatter index unbiased:

$$SI = \frac{\sqrt{\frac{1}{N}\sum_{i=1}^{N}(Y - X - BIAS)_i^2}}{\frac{1}{N}\sum_{i=1}^{N}|X_i|}$$

EV is the explained variance:

$$EV = \frac{\sum_{i=1}^{N}(X_i - \bar{X})^2 - \sum_{i=1}^{N}[(X_i - \bar{X}) - (Y_i - \bar{Y})]^2}{\sum_{i=1}^{N}(X_i - \bar{X})^2}$$

CC is the correlation coefficient:

$$CC = \frac{\sum_{i=1}^{N}(X_i - \bar{X})(Y_i - \bar{Y})}{\sqrt{\sum_{i=1}^{N}(X_i - \bar{X})^2 \sum_{i=1}^{N}(Y_i - \bar{Y})^2}}$$

PR is the peak ratio of N_p highest events:

$$PR = \frac{\sum_{i=1}^{N_p} Y_i}{\sum_{i=1}^{N_p} X_i}$$

Table 5. Summary of the quality indices for the validation of the model against data from Buoy I

	H_{m0}	$T_{z(Hm0 > 0.50\ m)}$
N	169630 (9.7 years)	140991 (8.0 years)
Y	1.17 m (94.4%)	4.35 s (95.6%)
BIAS	-0.07 m (-5.6%)	-0.18 s (-4.1%))
AME	0.18 m (14.7%)	0.39 s (8.6%)
RMSE	0.26 m (21.2%)	0.53 s (11.7%)
SI	0.20 (Unbiased)	0.11 (Unbiased)
EV	0.89	0.61
CC	0.94	0.84
PR	1.02 (N_p=19)	0.91 (N_p=16)

Table 6. Summary of the quality indices for the validation of the model against data from Buoy II

	H_{m0}	$T_{z(Hm0 > 0.50\ m)}$
N	13964 (290.9 days)	12325 (256.8 days)
Y	1.37 m (103.4%)	4.30 s (91.3%)
BIAS	0.04 m (3.4%)	-0.41 s (-8.7%))
AME	0.16 m (11.8%)	0.50 s (10.6%)
RMSE	0.22 m (16.3%)	0.63 s (13.4%)
SI	0.16 (Unbiased)	0.10 (Unbiased)
EV	0.93	0.80
CC	0.97	0.90
PR	0.98 (N_p=2)	0.91 (N_p=1)

Table 7. Summary of the quality indices for the validation of the model against data from Buoy III

	H_{m0}	$T_{z(Hm0 > 0.50\ m)}$
N	13443 (280.1 days)	12112 (252.3 days)
Y	1.46 m (99.8%)	4.47 s (91.2%)
BIAS	-0.00 m (-0.2%)	-0.43 s (-8.8%))
AME	0.16 m (10.7%)	0.53 s (10.9%)
RMSE	0.22 m (14.8%)	0.67 s (13.7%)
SI	0.15 (Unbiased)	0.10 (Unbiased)
EV	0.94	0.79
CC	0.97	0.89
PR	0.93 (N_p=2)	0.90 (N_p=16)

4. Forecast model

The forecast model for the DanWEC test site is based on the hindcast model where the grid output resolution is reduced as shown in Fig. 4. The forecast model updates a 5½ days-horizon twice every 24 hours [4]. The model forcing comprises input from regional DHI models and forecast wind fields. The list of output parameters for the forecast model are given in Tab. 8.

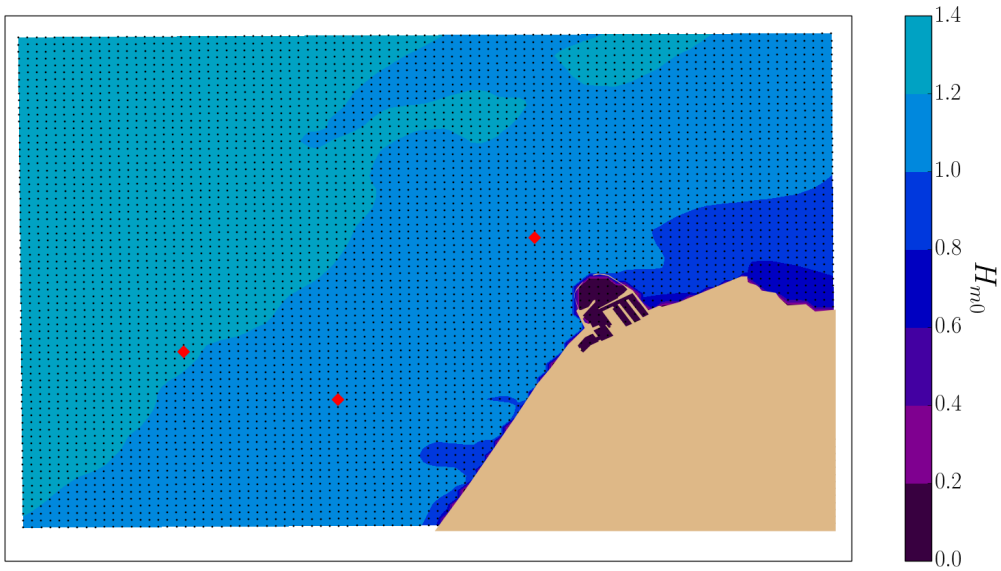

Fig. 4. Example of forecast H_{m0} for the total area provided for the forecast model at DanWEC. The three markers mark the position of the wave measuring buoys and the dots correspond to the mesh of the model, i.e. values for each point can be extracted.

Table 8. List of output parameters for the forecast model updated twice every 24 hours throughout the modelling area (Fig.4)

Parameter	Unit
H_{m0}	[m]
H_{max}	[m]
T_p	[s]
T_{01}	[s]
T_{02}	[s]
Wave direction	[°]
Wind speed	[m/s]
Current speed	[m/s]

4.1. Forecast model validation

In other to validate the forecast model, each forecast time series between the period January 2017 and December 2018 has been compared with observed data for the corresponding period. Figure 5 shows an example of a H_{m0} time series comparison between observed data and forecast data. Note that the first 12 hours correspond to hindcast data.

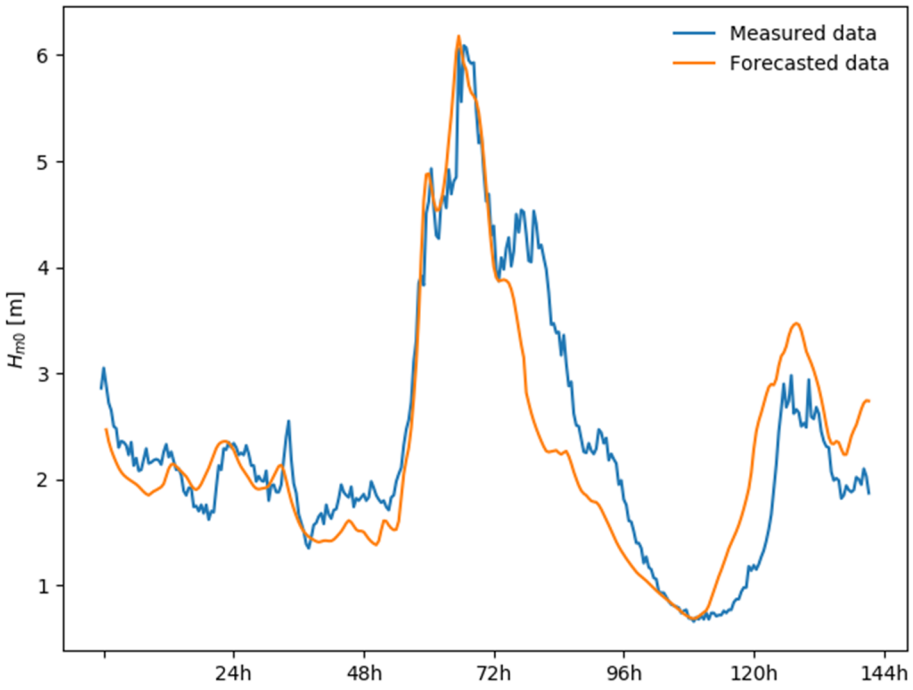

Fig. 5. Example of time series for measured values and forecast of H_{m0} over the whole forecast horizon.

In Fig. 6, the forecast horizon is divided into 4 timeframes, where the first 12 hours have been removed, and the forecasted data for H_{m0} is presented as a function of the observed data. *Horizon 1* corresponds to the timeframe [0, 36] hours, *Horizon 2* to]36, 72] hours, *Horizon 3* to]72, 108] hours and *Horizon 4* to]108, 144] hours. A 1:1 dotted-line is also shown in the figure to better qualify the agreement between the observed and forecasted data. The respective figure for T_p is presented in Fig. 7.

As expected for both H_{m0} and T_p, the prediction is better for the Horizon 1, corresponding to the first 36 hours. The second thing easy to notice is that the prediction for H_{m0} is more accurate than for T_p. It can also be noticed from Fig. 6 that there is a negative bias for large event, i.e. the model is somehow underpredicting high H_{m0} events. This effect is easier to appreciate further in the forecast horizon, especially Horizon 3 and 4.

For the accuracy analysis, the following error metrics have been used, defined in terms of the forecast data ($\hat{x}$), the observed data (x) and the number of validation points (N_v):

$\bar{\hat{x}}$ stands for the average of the forecast data $\hat{x}$:

$$\bar{\hat{x}} = \frac{1}{N_v}\sum_{i=1}^{N_v}\hat{x}_i$$

while $\bar{x}$ is the average of the observed data:

$$\bar{x} = \frac{1}{N_v}\sum_{i=1}^{N_v}x_i$$

AME is the absolute mean difference as defined previously:

$$AME = \frac{1}{N_v}\sum_{i=1}^{N_v}|\hat{x}_i - x_i|$$

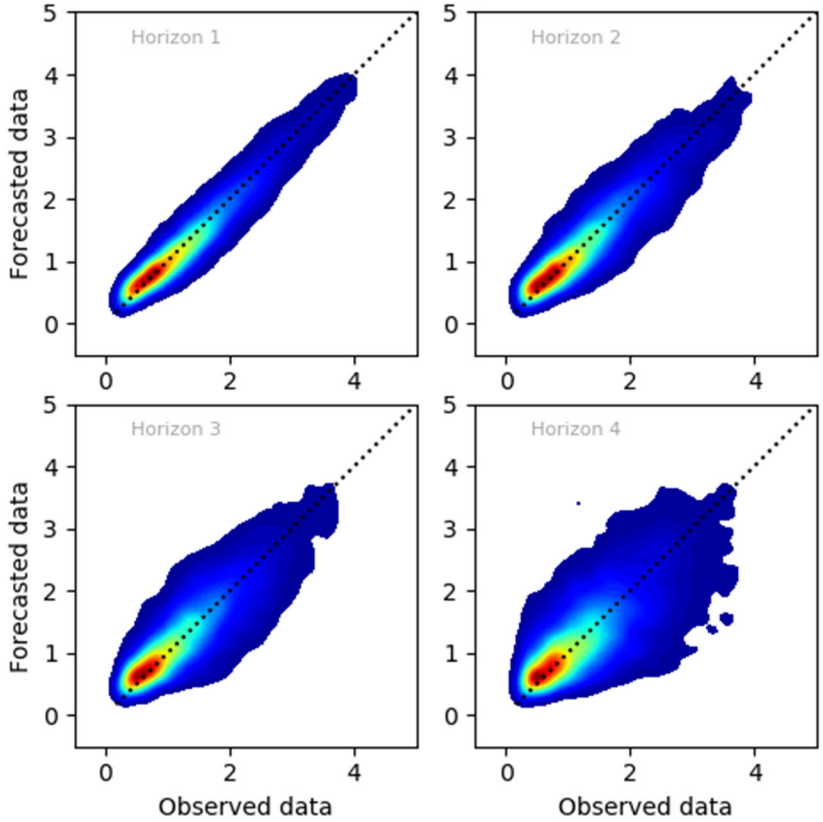

Fig. 6. Forecasted data as a function of observed data for H_{m0} for the total period corresponding to pair of points. The forecast horizon is divided into 4: *Horizon 1* corresponds to timeframe [0, 36] hours, *Horizon 2* to]36, 72] hours, *Horizon 3* to]72, 108] hours and *Horizon 4* to]108, 144] hours. The dotted line corresponds to a 1:1 line.

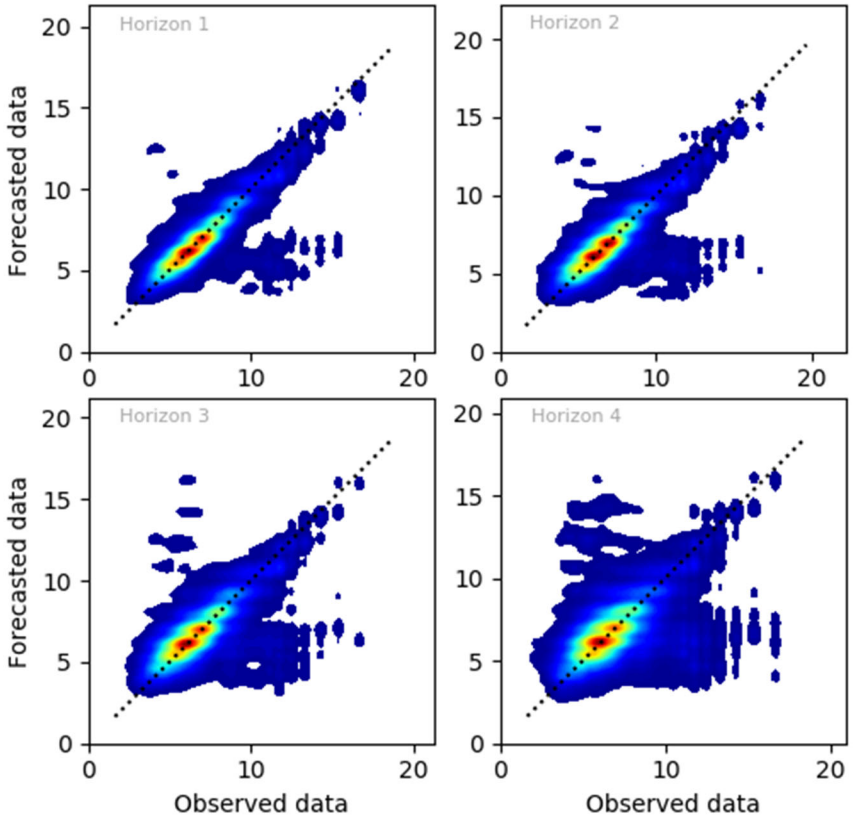

Fig. 7. Forecasted data as a function of observed data for T_p for the total period corresponding to pair of points. The forecast horizon is divided into 4: *Horizon 1* corresponds to timeframe [0, 36] hours, *Horizon 2* to]36, 72] hours, *Horizon 3* to]72, 108] hours and *Horizon 4* to]108, 144] hours. The dotted line corresponds to a 1:1 line.

MBE is the mean bias error:

$$MBE = \frac{1}{N_v}\sum_{i=1}^{N_v}(\hat{x}_i - x_i)$$

$RMSE$ is the root mean squared error:

$$RMSE = \sqrt{\frac{1}{N_v}\sum_{i=1}^{N_v}(\hat{x}_i - x_i)^2}$$

R^2 is the coefficient of determination:

$$R^2 = 1 - \frac{\sum_{i=1}^{N_v}(x_i - \hat{x}_i)^2}{\sum_{i=1}^{N_v}(x_i - \bar{x})^2}$$

SI is the scatter index:

$$SI = \frac{RMSE}{\bar{x}}$$

$MARE$ is mean absolute percentage error:

$$MARE = \frac{100}{N_v}\sum_{i=1}^{N_v}\left|\frac{x_i - \hat{x}_i}{x_i}\right|$$

$RRMSE$ is the relative root mean squared error:

$$RRMSE = \frac{100}{\bar{x}}\sqrt{\frac{1}{N_v}\sum_{i=1}^{N_v}(x_i - \hat{x}_i)^2}$$

$RMSRE$ is the root mean squared relative error:

$$RMSRE = \sqrt{\frac{1}{N_v}\sum_{i=1}^{N_v}\left(\frac{x_i - \hat{x}_i}{x_i}\right)^2}$$

All those error metrics were compiled as a function of the time horizon of the forecast. While AME, MBE and $RMSE$ have the same units as the observed/forecast parameter, R^2, SI, $MARE$, $RRMSE$ and $RMSRE$ are all relative error metrics and can thus be used to compare performance between different parameters.

Table 9 and 10 show the errors metrics for H_{m0} and T_p, respectively. One thing to notice from the tables is that the forecast model as a negative mean bias error, meaning that the model is predicting lower values of both H_{m0} and T_p throughout the forecast horizon, as it could also be seen in figure 6 and 7. The error metrics are also showing that the forecast model has higher accuracy the closer it is to the actual time. The model is also predicting more accurately wave heights than wave periods.

Those error metrics have been broken down into seasons and months to capture seasonal and monthly variations.

Table 9. Errors metrics for H_{m0} for the whole period, where $N_v = 424$.

	H_{m0} $(N_v = 424)$							
	AME	MBE	$RMSE$	R^2	SI	$MARE$	$RRMSE$	$RMSRE$
	[m]	[m]	[m]	[-]	[-]	[%]	[%]	[-]
18h	0.169	-0.045	0.239	0.929	0.151	11.720	15.083	0.154
36h	0.209	-0.042	0.287	0.902	0.181	14.502	18.111	0.199
54h	0.281	-0.058	0.428	0.778	0.271	18.669	27.061	0.262
72h	0.323	-0.070	0.503	0.704	0.318	21.101	31.750	0.289
90h	0.351	-0.042	0.514	0.673	0.327	23.581	32.691	0.335
108h	0.367	-0.052	0.528	0.653	0.336	25.947	33.609	0.360
126h	0.444	-0.031	0.639	0.487	0.409	32.819	40.909	0.489
144h	0.509	-0.056	0.690	0.353	0.446	38.187	44.556	0.588

Table 10. Errors metrics for T_p for the whole period, where $N_v = 424$.

	T_p $(N_v = 424)$							
	AME	MBE	$RMSE$	R^2	SI	$MARE$	$RRMSE$	$RMSRE$
	[s]	[s]	[s]	[-]	[-]	[%]	[%]	[-]
18h	1.132	-0.192	2.096	0.327	0.266	14.111	26.618	0.267
36h	1.215	-0.083	2.323	0.230	0.297	16.595	29.655	0.353
54h	1.390	-0.269	2.419	0.158	0.306	17.453	30.637	0.307
72h	1.306	-0.210	2.297	0.257	0.293	16.853	29.274	0.295
90h	1.651	-0.085	2.755	-0.176	0.352	21.674	35.192	0.382
108h	1.751	-0.099	2.932	-0.199	0.372	22.791	37.231	0.398
126h	1.844	-0.190	2.902	-0.257	0.371	23.861	37.096	0.386
144h	1.919	-0.242	2.959	-0.218	0.376	24.509	37.649	0.390

4.1.1. Seasonal variations

The time series were divided into seasons to grasp seasonal variations for the forecast model. The seasons are divided according to the following: winter includes the months of December, January and February; spring includes the months of March, April and May; summer includes the months of June, July and August; and includes the months of September, October and November. Figures 8 and 9 show the equivalent of Fig. 6 and 7 for the winter season and Tab. 11 and 12 show the error metrics for the winter season.

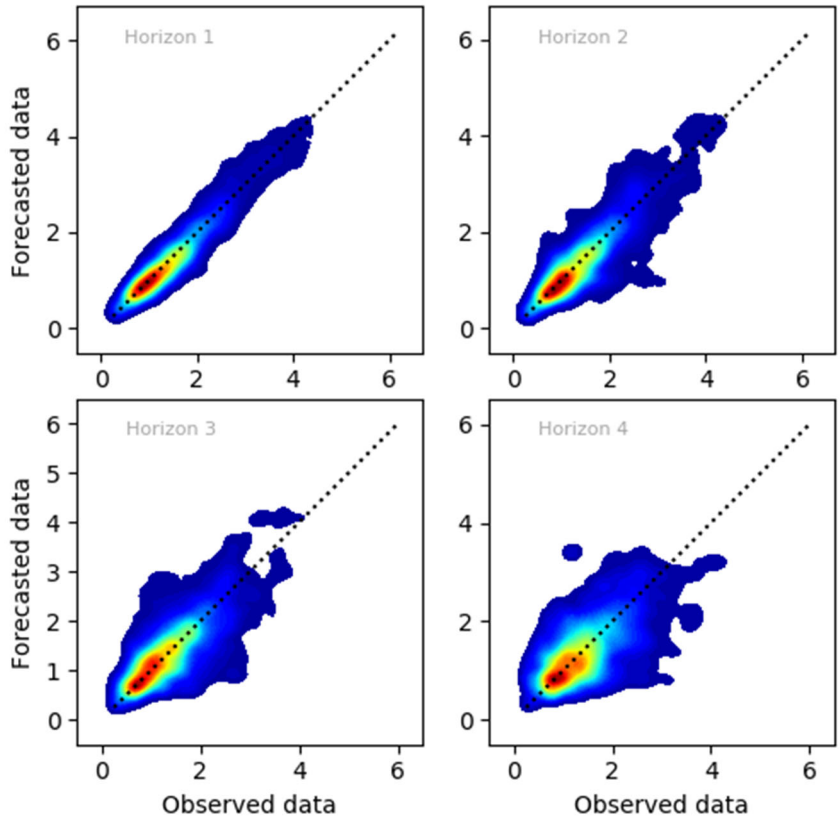

Fig. 8. Forecasted data as a function of observed data for H_{m0} for the winter months. The forecast horizon is divided into 4: *Horizon 1* corresponds to timeframe [0, 36] hours, *Horizon 2* to]36, 72] hours, *Horizon 3* to]72, 108] hours and *Horizon 4* to]108, 144] hours. The dotted line corresponds to a 1:1 line.

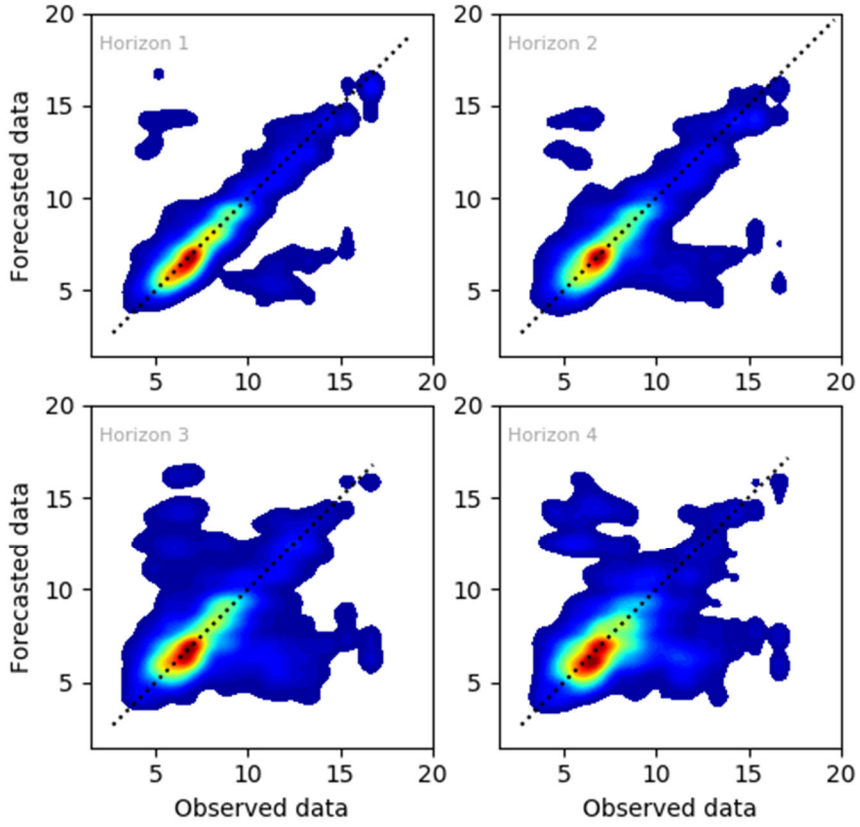

Fig. 9. Forecasted data as a function of observed data for T_p for the winter months. The forecast horizon is divided into 4: *Horizon 1* corresponds to timeframe [0, 36] hours, *Horizon 2* to]36, 72] hours, *Horizon 3* to]72, 108] hours and *Horizon 4* to]108, 144] hours. The dotted line corresponds to a 1:1 line.

Table 11. Errors metrics for H_{m0} for the winter period, where $N_v = 228$.

	H_{m0} ($N_v = 228$)							
	AME	MBE	$RMSE$	R^2	SI	$MARE$	$RRMSE$	$RMSRE$
	[m]	[m]	[m]	[-]	[-]	[%]	[%]	[-]
18h	0.167	-0.034	0.246	0.936	0.150	10.650	15.030	0.137
36h	0.206	-0.028	0.283	0.919	0.173	13.976	17.333	0.199
54h	0.318	-0.077	0.493	0.748	0.299	19.887	29.887	0.279
72h	0.371	-0.088	0.606	0.637	0.365	22.276	36.479	0.313
90h	0.399	-0.074	0.591	0.616	0.360	24.728	36.004	0.346
108h	0.390	-0.069	0.582	0.616	0.361	26.906	36.126	0.374
126h	0.463	-0.043	0.671	0.485	0.418	33.817	41.819	0.514
144h	0.502	-0.070	0.666	0.414	0.416	36.696	41.634	0.522

Table 10. Errors metrics for T_p for the winter period, where $N_v = 228$.

	T_p ($N_v = 228$)							
	AME	MBE	$RMSE$	R^2	SI	$MARE$	$RRMSE$	$RMSRE$
	[s]	[s]	[s]	[-]	[-]	[%]	[%]	[-]
18h	1.247	-0.296	2.283	0.259	0.275	14.571	27.481	0.273
36h	1.309	-0.133	2.482	0.211	0.303	17.073	30.257	0.349
54h	1.520	-0.315	2.579	0.093	0.312	18.682	31.244	0.325
72h	1.475	-0.318	2.546	0.180	0.309	17.576	30.881	0.287
90h	1.790	-0.106	2.843	-0.238	0.346	22.912	34.614	0.382
108h	2.116	-0.322	3.359	-0.441	0.406	25.959	40.592	0.428
126h	1.917	-0.242	2.930	-0.242	0.363	24.042	36.273	0.388
144h	2.176	-0.332	3.241	-0.383	0.396	27.504	39.640	0.438

Tables 11 and 12 show the same tendencies as seen previously for the whole period (Tab. 9 and 10). A negative mean bias error, a forecast less accurate as getting further into the horizon and a forecast model better at predicting H_{m0} than T_p. The values of the error metrics resemble closely the values obtained for the whole period.

Figures 10 and 11 show the equivalent of Fig. 6 and 7 for the spring season and Tab. 13 and 14 show the error metrics for the spring season.

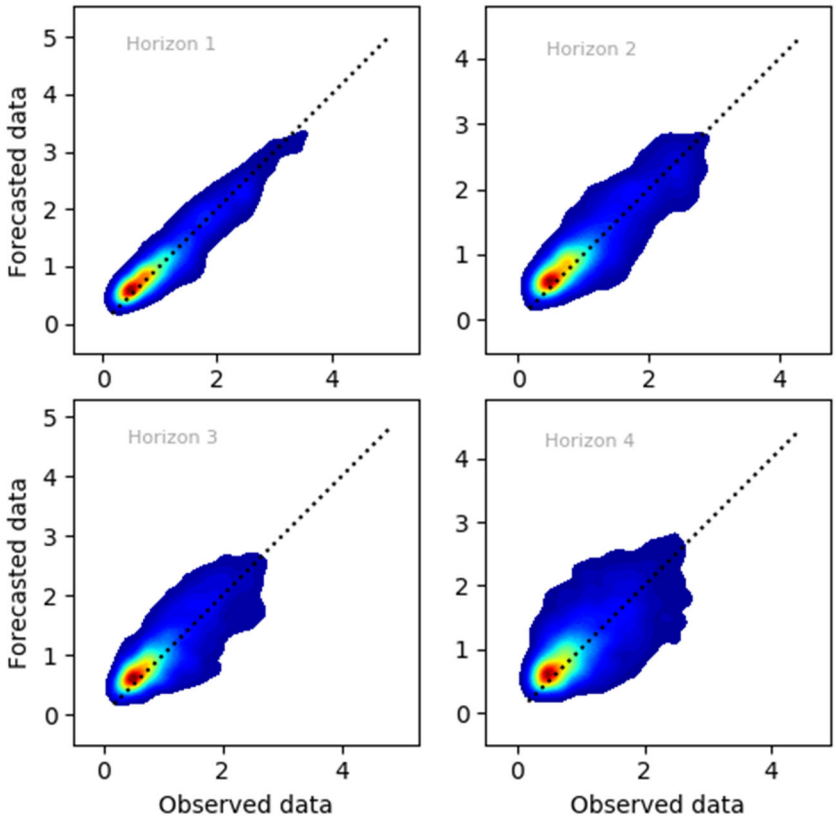

Fig. 10. Forecasted data as a function of observed data for H_{m0} for the spring months. The forecast horizon is divided into 4: *Horizon 1* corresponds to timeframe [0, 36] hours, *Horizon 2* to]36, 72] hours, *Horizon 3* to]72, 108] hours and *Horizon 4* to]108, 144] hours. The dotted line corresponds to a 1:1 line.

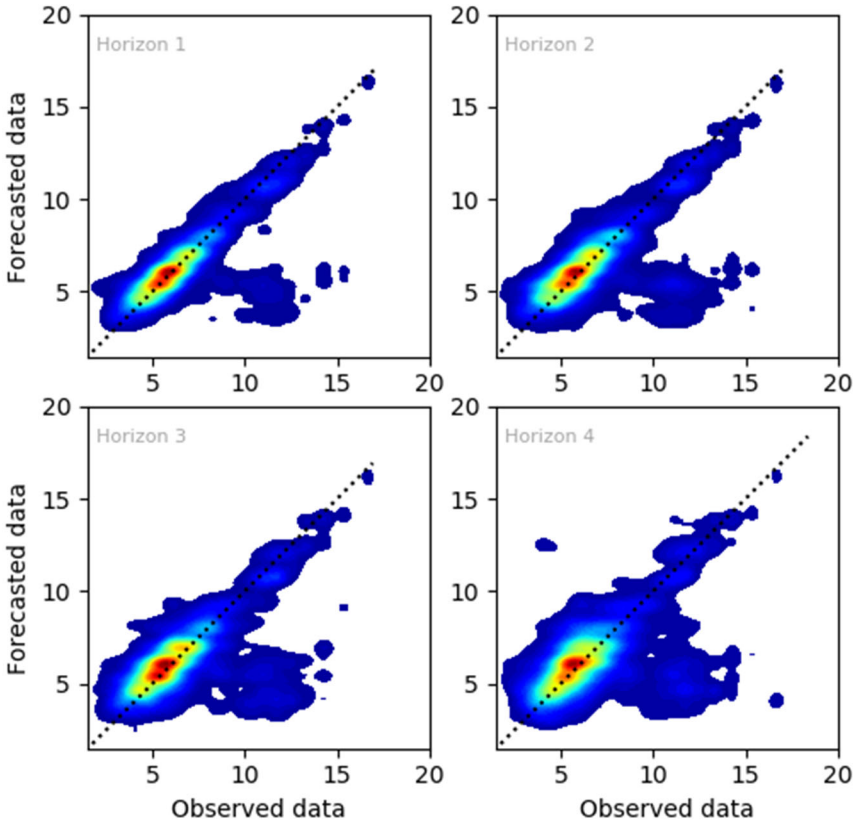

Fig. 11. Forecasted data as a function of observed data for T_p for the spring months. The forecast horizon is divided into 4: *Horizon 1* corresponds to timeframe [0, 36] hours, *Horizon 2* to]36, 72] hours, *Horizon 3* to]72, 108] hours and *Horizon 4* to]108, 144] hours. The dotted line corresponds to a 1:1 line.

Table 13. Errors metrics for H_{m0} for the spring period, where $N_v = 322$.

H_{m0} ($N_v = 322$)								
	AME	MBE	$RMSE$	R^2	SI	$MARE$	$RRMSE$	$RMSRE$
	[m]	[m]	[m]	[-]	[-]	[%]	[%]	[-]
18h	0.168	0.002	0.219	0.925	0.185	19.279	18.484	0.283
36h	0.186	0.011	0.249	0.888	0.214	20.172	21.439	0.276
54h	0.225	0.038	0.320	0.835	0.278	24.989	27.801	0.357
72h	0.263	0.026	0.358	0.753	0.318	28.016	31.842	0.393
90h	0.293	0.043	0.413	0.714	0.366	32.998	36.643	0.489
108h	0.307	0.028	0.437	0.652	0.385	32.076	38.508	0.457
126h	0.379	0.049	0.548	0.502	0.483	41.684	48.282	0.684
144h	0.414	0.050	0.600	0.314	0.539	46.039	53.924	0.764

Table 14. Errors metrics for T_p for the spring period, where $N_v = 322$.

T_p ($N_v = 322$)								
	AME	MBE	$RMSE$	R^2	SI	$MARE$	$RRMSE$	$RMSRE$
	[s]	[s]	[s]	[-]	[-]	[%]	[%]	[-]
18h	1.248	-0.477	2.332	0.362	0.328	17.572	32.759	0.328
36h	1.103	-0.349	2.023	0.499	0.292	15.450	29.231	0.243
54h	1.412	-0.508	2.452	0.255	0.347	20.120	34.676	0.350
72h	1.300	-0.188	2.195	0.367	0.321	20.008	32.127	0.331
90h	1.526	-0.588	2.543	0.260	0.358	21.123	35.797	0.328
108h	1.472	-0.456	2.540	0.258	0.366	20.390	36.581	0.317
126h	1.663	-0.534	2.612	0.219	0.365	22.727	36.502	0.323
144h	1.743	-0.230	2.902	0.066	0.413	25.035	41.271	0.408

Again, the tendencies seen previously can be seen in Tab. 13 and 14, apart from the positive mean bias error for H_{m0}. The values of the error metrics show that the model is less performing for the spring season.

Figures 12 and 13 show the equivalent of Fig. 6 and 7 for the summer season and Tab. 15 and 16 show the error metrics for the summer season.

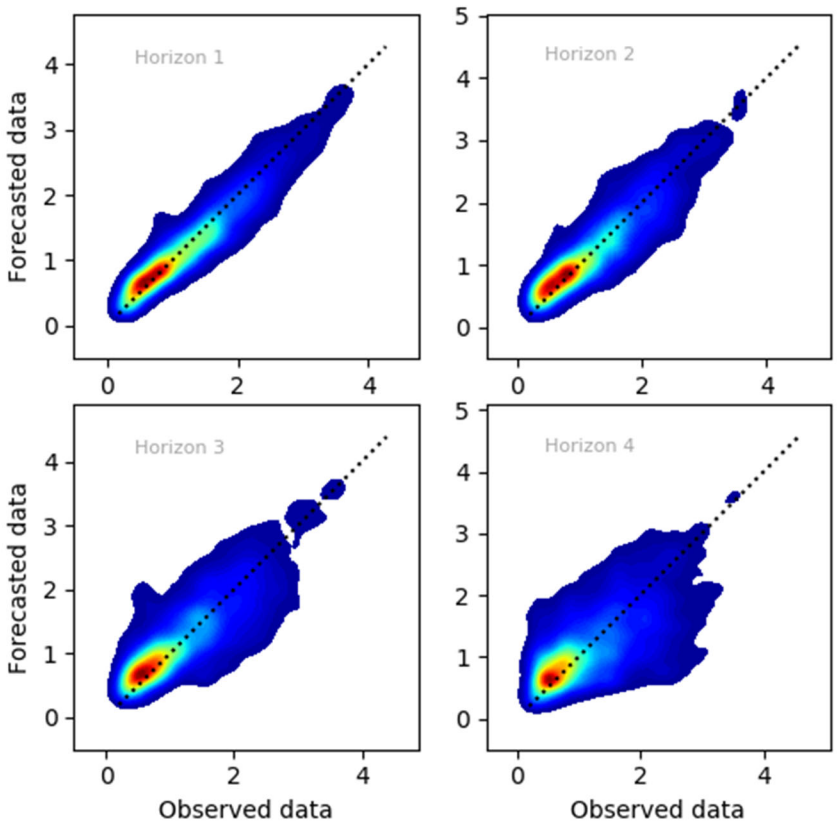

Fig. 12. Forecasted data as a function of observed data for H_{m0} for the summer months. The forecast horizon is divided into 4: *Horizon 1* corresponds to timeframe [0, 36] hours, *Horizon 2* to]36, 72] hours, *Horizon 3* to]72, 108] hours and *Horizon 4* to]108, 144] hours. The dotted line corresponds to a 1:1 line.

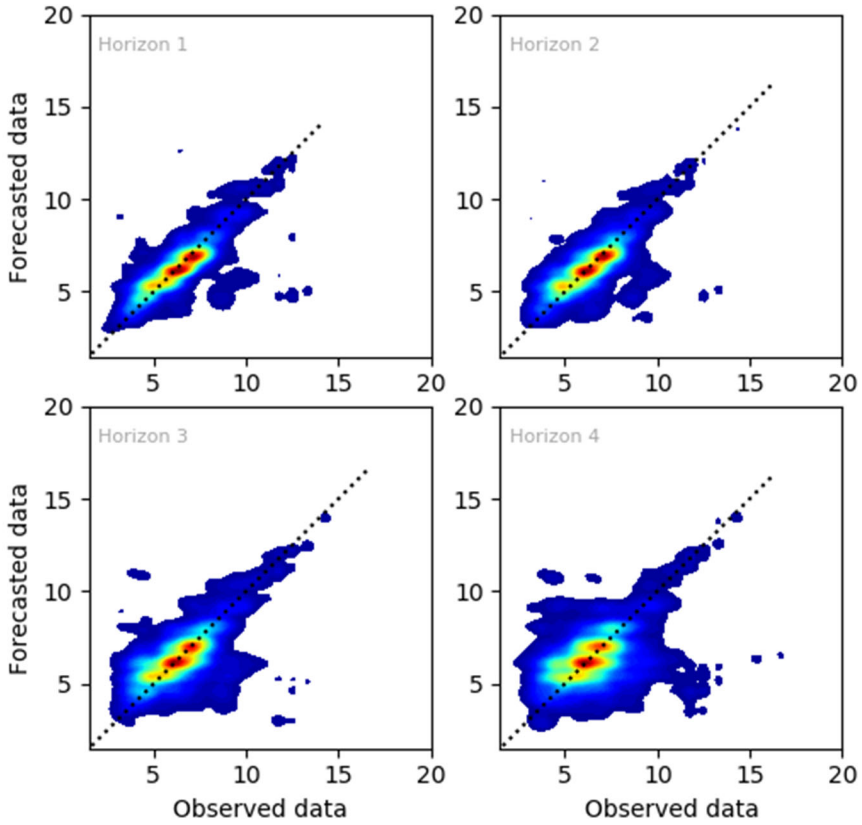

Fig. 13. Forecasted data as a function of observed data for T_p for the summer months. The forecast horizon is divided into 4: *Horizon 1* corresponds to timeframe [0, 36] hours, *Horizon 2* to]36, 72] hours, *Horizon 3* to]72, 108] hours and *Horizon 4* to]108, 144] hours. The dotted line corresponds to a 1:1 line.

Table 15. Errors metrics for H_{m0} for the summer period, where $N_v = 263$.

H_{m0} ($N_v = 263$)								
	AME	MBE	$RMSE$	R^2	SI	$MARE$	$RRMSE$	$RMSRE$
	[m]	[m]	[m]	[-]	[-]	[%]	[%]	[-]
18h	0.140	-0.029	0.187	0.939	0.146	13.558	14.628	0.188
36h	0.195	-0.045	0.264	0.874	0.205	17.428	20.539	0.237
54h	0.211	0.010	0.287	0.854	0.222	20.346	22.161	0.307
72h	0.247	0.016	0.338	0.793	0.264	23.808	26.364	0.369
90h	0.300	0.027	0.426	0.697	0.329	28.560	32.904	0.432
108h	0.339	-0.003	0.478	0.616	0.367	32.169	36.697	0.515
126h	0.399	-0.041	0.566	0.476	0.434	37.642	43.448	0.615
144h	0.486	-0.042	0.676	0.239	0.525	48.506	52.512	0.806

Table 16. Errors metrics for T_p for the summer period, where $N_v = 263$.

T_p ($N_v = 263$)								
	AME	MBE	$RMSE$	R^2	SI	$MARE$	$RRMSE$	$RMSRE$
	[s]	[s]	[s]	[-]	[-]	[%]	[%]	[-]
18h	0.776	-0.087	1.375	0.482	0.214	12.168	21.396	0.193
36h	0.778	-0.073	1.326	0.450	0.204	12.643	20.427	0.222
54h	0.908	-0.104	1.444	0.433	0.222	14.231	22.168	0.210
72h	0.943	0.026	1.503	0.405	0.228	15.633	22.774	0.264
90h	1.139	-0.137	1.837	0.146	0.279	18.107	27.907	0.281
108h	1.180	-0.146	1.879	0.145	0.281	18.557	28.065	0.293
126h	1.365	-0.108	2.031	-0.040	0.308	22.194	30.752	0.338
144h	1.457	-0.133	2.159	-0.069	0.321	23.891	32.123	0.382

For the summer period, the mean bias error is not only negative: it oscillates between [- 0.045, 0.027] m for H_{m0} and [- 0.146, 0.026] s for T_p. The error metric values are also showing that the forecast model is performing better for this period with respect to the whole period and the spring and winter periods.

Figures 14 and 15 show the equivalent of Fig. 6 and 7 for the autumn season and Tab. 17 and 18 show the error metrics for the autumn season.

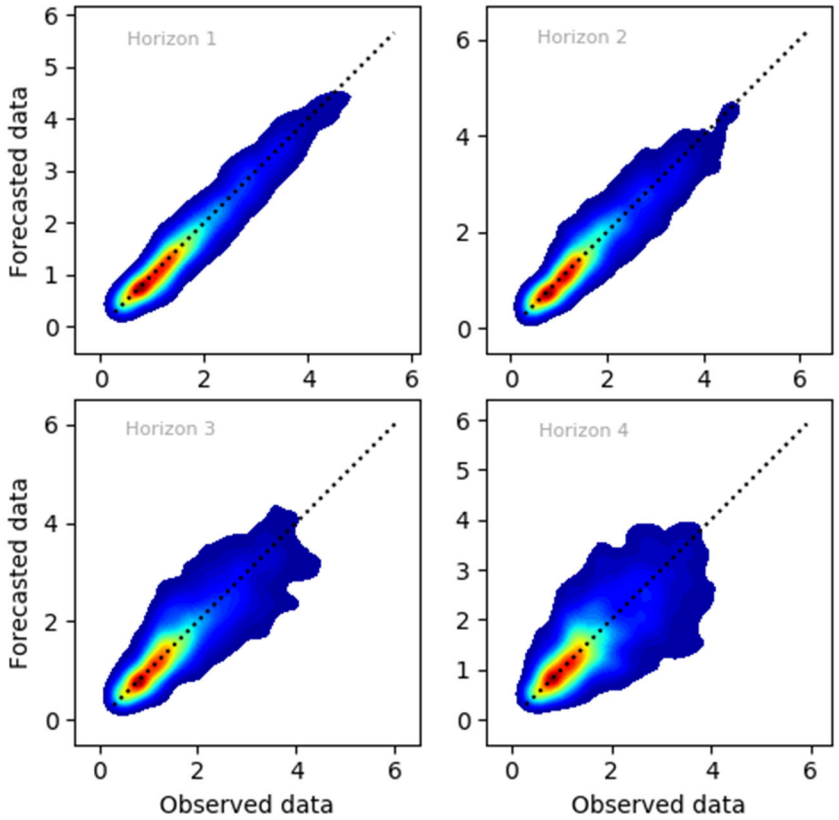

Fig. 14. Forecasted data as a function of observed data for H_{m0} for the autumn months. The forecast horizon is divided into 4: *Horizon 1* corresponds to timeframe [0, 36] hours, *Horizon 2* to]36, 72] hours, *Horizon 3* to]72, 108] hours and *Horizon 4* to]108, 144] hours. The dotted line corresponds to a 1:1 line.

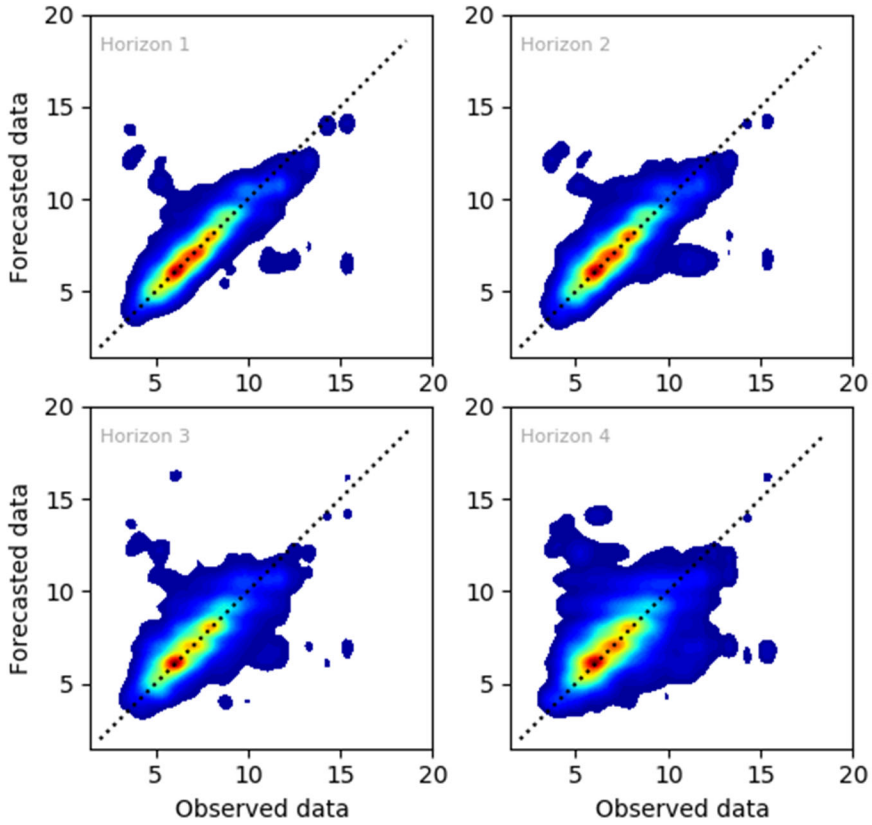

Fig. 15. Forecasted data as a function of observed data for T_p for the autumn months. The forecast horizon is divided into 4: *Horizon 1* corresponds to timeframe [0, 36] hours, *Horizon 2* to]36, 72] hours, *Horizon 3* to]72, 108] hours and *Horizon 4* to]108, 144] hours. The dotted line corresponds to a 1:1 line.

Table 17. Errors metrics for H_{m0} for the autumn period, where $N_v = 330$.

	H_{m0} $(N_v = 330)$							
	AME	MBE	$RMSE$	R^2	SI	$MARE$	$RRMSE$	$RMSRE$
	[m]	[m]	[m]	[-]	[-]	[%]	[%]	[-]
18h	0.167	-0.066	0.230	0.946	0.140	11.782	13.966	0.155
36h	0.200	-0.073	0.279	0.917	0.170	13.402	16.954	0.176
54h	0.241	-0.037	0.364	0.858	0.223	15.664	22.261	0.218
72h	0.264	-0.043	0.379	0.847	0.230	17.472	22.995	0.238
90h	0.298	-0.021	0.440	0.799	0.265	18.807	26.457	0.267
108h	0.367	-0.050	0.517	0.720	0.309	23.070	30.856	0.313
126h	0.420	-0.089	0.619	0.602	0.369	26.698	36.856	0.389
144h	0.496	-0.111	0.712	0.477	0.419	30.444	41.901	0.422

Table 18. Errors metrics for T_p for the autumn period, where $N_v = 330$.

	T_p $(N_v = 330)$							
	AME	MBE	$RMSE$	R^2	SI	$MARE$	$RRMSE$	$RMSRE$
	[m]	[m]	[m]	[-]	[-]	[%]	[%]	[-]
18h	0.947	-0.097	1.736	0.502	0.227	12.588	22.725	0.234
36h	0.999	0.027	1.901	0.363	0.251	14.234	25.128	0.309
54h	1.070	-0.082	1.897	0.413	0.250	14.131	24.963	0.253
72h	1.099	0.071	1.901	0.347	0.252	16.024	25.239	0.305
90h	1.417	0.001	2.494	-0.060	0.330	19.146	33.037	0.358
108h	1.255	0.084	2.022	0.236	0.269	17.975	26.904	0.319
126h	1.611	0.040	2.644	-0.190	0.350	21.953	34.997	0.368
144h	1.541	0.132	2.335	-0.071	0.313	22.583	31.311	0.375

For the autumn season, the mean bias error for H_{m0} follows the trend seen for the whole period while the mean bias error for T_p is mostly positive. The values of the error metrics show that the model is performing better for this season than all other seasons.

The variation of the $RRMSE$ on a seasonal basis is depicted in Fig. 16 and 17 for H_{m0} and T_p respectively. The $RRMSE$ is shown as a function of the forecast horizon for the four seasons and for all the data points. According to [12] the forecast is considered good if $RRMSE$ <20%, fair if 20% < $RRMSE$ < 30%, and poor if $RRMSE$ > 30%. The gray area on the figures can be considered as the limit of accuracy for the forecast model. It is again easy to notice that the model is more accurate in predicting wave heights than wave periods. The summer and autumn seasons of the last two years have been relatively calm. With this in mind, it can also be seen from Fig. 16 and 17 that the forecast model can better predict milder wave climate, as both H_{m0} and T_p can be fairly predicted as far as 4.5 days ahead for those two seasons.

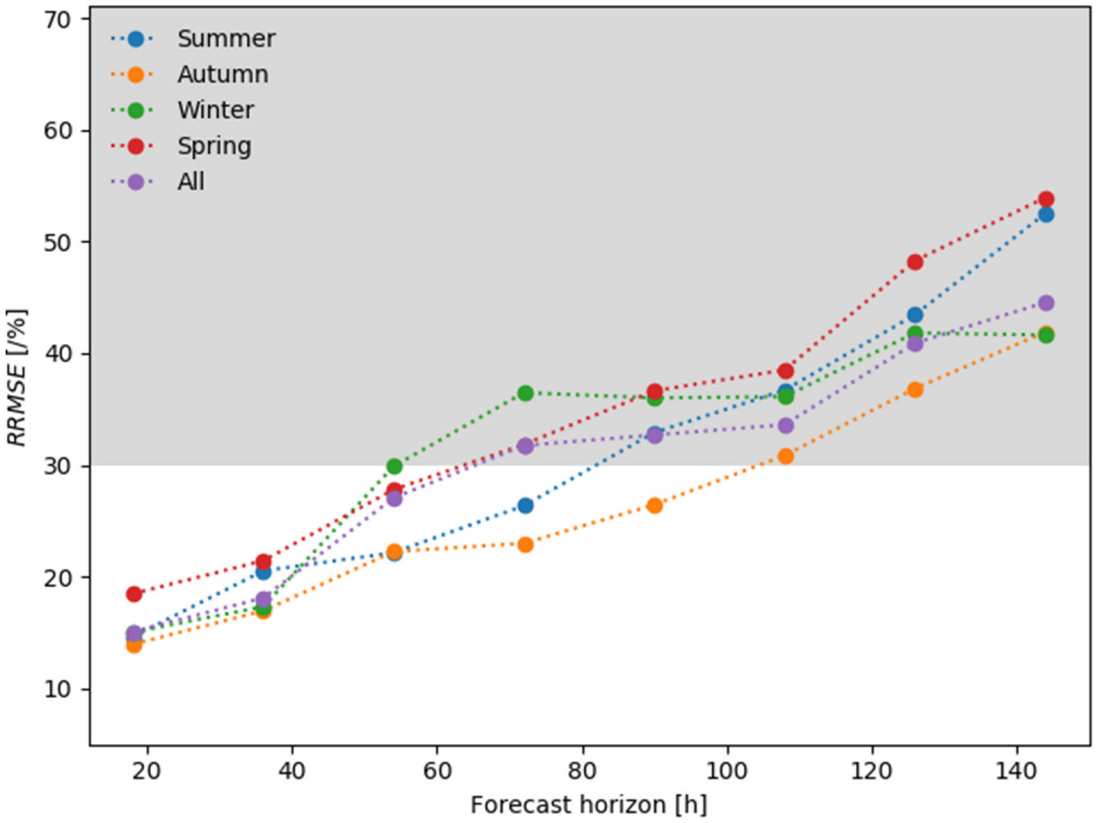

Fig. 16. *RRMSE* of H_{m0} as a function of the forecast horizon for the four seasons. The *RRMSE* as a function of the forecast horizon for the whole period is also shown. The grey area can be considered as the limit of accuracy for the forecast model.

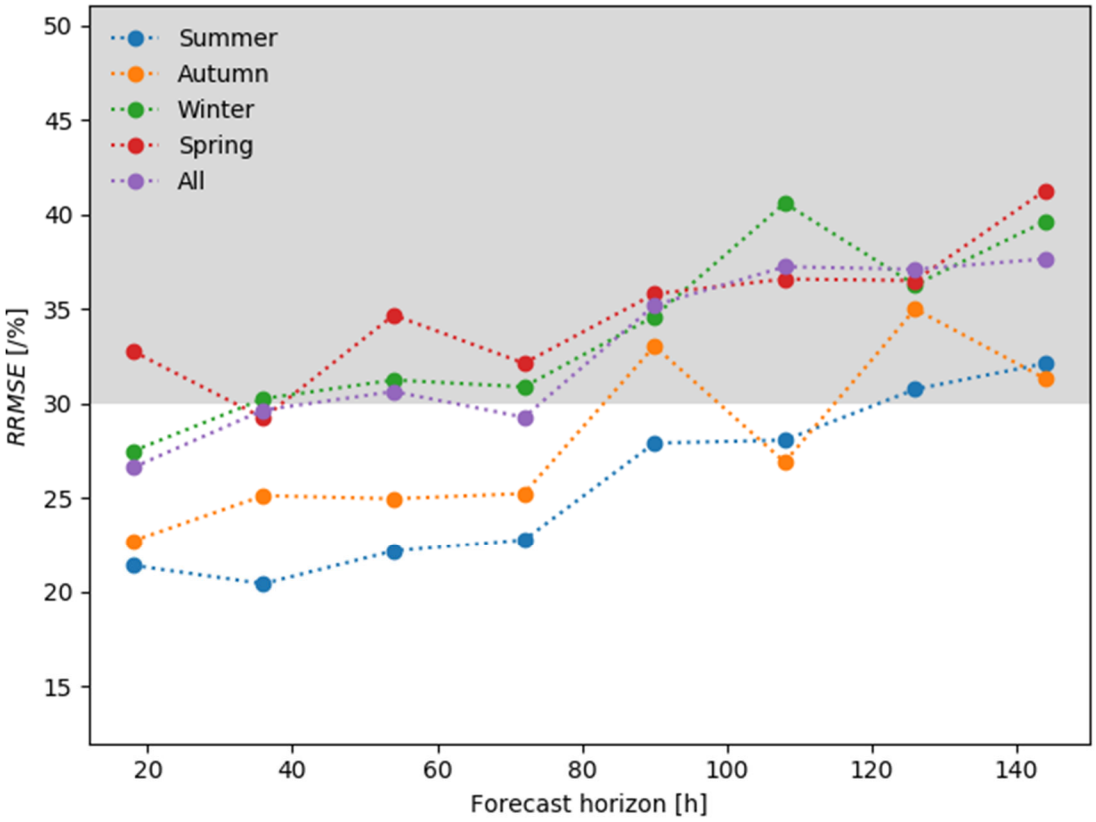

Fig. 17. *RRMSE* of T_p as a function of the forecast horizon for the four seasons. The *RRMSE* as a function of the forecast horizon for the whole period is also shown. The grey area can be considered as the limit of accuracy for the forecast model.

4.1.2. Monthly variations

The error metrics were also obtained for each month. All results are compiled in Tab. 19 to 42 for the 12 months and for both H_{m0} et T_p.

Table 19. Errors metrics for H_{m0} for the month of January, where $N_v = 105$.

H_{m0} $(N_v = 105)$								
	AME	MBE	$RMSE$	R^2	SI	$MARE$	$RRMSE$	$RMSRE$
	[m]	[m]	[m]	[-]	[-]	[%]	[%]	[-]
18h	0.176	-0.021	0.247	0.934	0.147	10.802	14.682	0.139
36h	0.180	-0.019	0.236	0.950	0.143	12.623	14.286	0.163
54h	0.277	-0.026	0.434	0.814	0.260	17.749	26.046	0.242
72h	0.264	-0.021	0.399	0.862	0.240	16.696	24.026	0.225
90h	0.323	0.016	0.458	0.756	0.286	20.992	28.562	0.293
108h	0.314	0.006	0.435	0.796	0.278	23.035	27.756	0.318
126h	0.407	0.065	0.583	0.596	0.379	31.130	37.886	0.482
144h	0.485	0.073	0.598	0.538	0.396	39.460	39.555	0.557

Table 20. Errors metrics for T_p for the month of January, where $N_v = 105$.

T_p $(N_v = 105)$								
	AME	MBE	$RMSE$	R^2	SI	$MARE$	$RRMSE$	$RMSRE$
	[m]	[m]	[m]	[-]	[-]	[%]	[%]	[-]
18h	1.544	-0.703	2.651	0.071	0.311	16.108	31.117	0.242
36h	1.389	-0.481	2.588	0.171	0.311	16.435	31.094	0.314
54h	1.904	-0.716	3.171	-0.137	0.372	21.336	37.224	0.346
72h	1.657	-0.407	2.966	-0.074	0.358	18.841	35.840	0.326
90h	1.994	-0.397	3.175	-0.182	0.380	23.540	37.982	0.365
108h	2.371	-0.290	3.615	-0.596	0.440	29.446	43.958	0.471
126h	2.294	-0.540	3.375	-0.285	0.406	27.314	40.632	0.422
144h	2.536	-0.066	3.723	-0.607	0.447	32.318	44.659	0.514

Table 21. Errors metrics for H_{m0} for the month of February, where $N_v = 83$.

H_{m0} ($N_v = 83$)								
	AME	MBE	$RMSE$	R^2	SI	$MARE$	$RRMSE$	$RMSRE$
	[m]	[m]	[m]	[-]	[-]	[%]	[%]	[-]
18h	0.180	-0.058	0.279	0.916	0.187	12.011	18.688	0.151
36h	0.202	-0.033	0.277	0.899	0.187	15.108	18.704	0.238
54h	0.248	-0.023	0.352	0.852	0.232	17.231	23.245	0.221
72h	0.313	-0.021	0.447	0.725	0.298	21.959	29.769	0.305
90h	0.325	-0.111	0.444	0.774	0.289	22.066	28.902	0.273
108h	0.332	-0.055	0.410	0.766	0.271	27.743	27.103	0.402
126h	0.379	-0.065	0.507	0.687	0.329	33.085	32.875	0.546
144h	0.386	-0.125	0.513	0.610	0.322	28.281	32.204	0.420

Table 22. Errors metrics for T_p for the month of February, where $N_v = 83$.

T_p ($N_v = 83$)								
	AME	MBE	$RMSE$	R^2	SI	$MARE$	$RRMSE$	$RMSRE$
	[m]	[m]	[m]	[-]	[-]	[%]	[%]	[-]
18h	1.001	0.346	1.870	0.553	0.231	14.976	23.115	0.344
36h	1.390	0.147	2.684	0.226	0.319	19.597	31.923	0.432
54h	1.152	0.046	1.962	0.498	0.242	16.030	24.200	0.323
72h	1.165	-0.270	1.977	0.575	0.236	14.023	23.629	0.206
90h	1.511	0.381	2.586	-0.137	0.322	21.976	32.205	0.425
108h	1.937	-0.349	3.334	-0.211	0.396	23.422	39.644	0.417
126h	1.536	0.002	2.554	-0.052	0.328	21.194	32.793	0.380
144h	1.570	-0.691	2.444	0.226	0.301	18.963	30.114	0.301

Table 23. Errors metrics for H_{m0} for the month of March, where $N_v = 80$.

H_{m0} ($N_v = 80$)								
	AME	MBE	$RMSE$	R^2	SI	$MARE$	$RRMSE$	$RMSRE$
	[m]	[m]	[m]	[-]	[-]	[%]	[%]	[-]
18h	0.203	-0.061	0.262	0.866	0.186	17.190	18.611	0.223
36h	0.233	-0.037	0.297	0.827	0.214	18.819	21.413	0.238
54h	0.256	-0.036	0.342	0.773	0.247	20.057	24.693	0.262
72h	0.325	-0.064	0.425	0.610	0.314	26.307	31.390	0.346
90h	0.326	-0.043	0.418	0.636	0.309	27.885	30.927	0.378
108h	0.382	-0.066	0.485	0.575	0.342	31.599	34.236	0.417
126h	0.481	0.016	0.651	0.183	0.474	40.330	47.384	0.559
144h	0.537	-0.014	0.735	-0.084	0.551	51.075	55.110	0.874

Table 24. Errors metrics for T_p for the month of March, where $N_v = 80$.

T_p ($N_v = 80$)								
	AME	MBE	$RMSE$	R^2	SI	$MARE$	$RRMSE$	$RMSRE$
	[m]	[m]	[m]	[-]	[-]	[%]	[%]	[-]
18h	0.890	-0.433	1.640	0.321	0.233	11.205	23.321	0.174
36h	0.943	-0.421	1.803	0.493	0.252	11.636	25.154	0.173
54h	1.117	-0.632	2.070	-0.010	0.292	13.546	29.183	0.208
72h	1.219	-0.429	2.102	0.192	0.299	15.593	29.896	0.225
90h	1.151	-0.525	1.914	0.131	0.272	14.979	27.246	0.218
108h	1.371	-0.338	2.527	-0.067	0.354	17.073	35.437	0.256
126h	1.618	-0.432	2.336	-0.151	0.322	22.256	32.249	0.314
144h	1.803	-0.465	2.828	-0.058	0.387	22.142	38.703	0.303

Table 25. Errors metrics for H_{m0} for the month of April, where $N_v = 111$.

H_{m0} $(N_v = 111)$								
	AME	MBE	$RMSE$	R^2	SI	$MARE$	$RRMSE$	$RMSRE$
	[m]	[m]	[m]	[-]	[-]	[%]	[%]	[-]
18h	0.149	-0.004	0.192	0.957	0.136	15.383	13.637	0.260
36h	0.188	0.003	0.266	0.897	0.199	17.122	19.871	0.239
54h	0.204	0.033	0.303	0.883	0.220	19.309	22.025	0.300
72h	0.268	0.061	0.370	0.787	0.285	26.785	28.542	0.418
90h	0.300	0.048	0.430	0.760	0.326	31.082	32.628	0.526
108h	0.344	0.091	0.502	0.603	0.396	33.469	39.591	0.534
126h	0.384	0.105	0.548	0.585	0.429	43.093	42.894	0.865
144h	0.386	0.093	0.547	0.505	0.447	43.289	44.674	0.732

Table 26. Errors metrics for T_p for the month of April, where $N_v = 111$.

T_p $(N_v = 111)$								
	AME	MBE	$RMSE$	R^2	SI	$MARE$	$RRMSE$	$RMSRE$
	[m]	[m]	[m]	[-]	[-]	[%]	[%]	[-]
18h	1.355	-0.191	2.417	0.209	0.346	21.628	34.630	0.429
36h	1.060	-0.096	1.705	0.521	0.256	16.940	25.621	0.273
54h	1.331	-0.031	2.244	0.229	0.333	21.406	33.332	0.373
72h	1.123	0.119	1.621	0.472	0.251	20.182	25.057	0.330
90h	1.475	-0.427	2.512	0.130	0.364	20.994	36.423	0.327
108h	1.268	-0.028	2.023	0.423	0.304	20.274	30.379	0.304
126h	1.473	-0.293	2.390	0.122	0.355	21.754	35.494	0.312
144h	1.989	0.202	3.321	-0.521	0.496	32.574	49.638	0.570

Table 27. Errors metrics for H_{m0} for the month of May, where $N_v = 119$.

H_{m0} ($N_v = 119$)								
	AME	MBE	$RMSE$	R^2	SI	$MARE$	$RRMSE$	$RMSRE$
	[m]	[m]	[m]	[-]	[-]	[%]	[%]	[-]
18h	0.166	0.049	0.215	0.876	0.257	24.944	25.675	0.343
36h	0.155	0.038	0.194	0.887	0.229	24.164	22.891	0.331
54h	0.218	0.072	0.317	0.742	0.391	32.735	39.150	0.442
72h	0.216	0.033	0.294	0.747	0.353	29.814	35.299	0.396
90h	0.262	0.082	0.393	0.615	0.475	37.708	47.527	0.518
108h	0.235	0.023	0.344	0.672	0.400	31.658	40.045	0.415
126h	0.304	0.025	0.460	0.481	0.535	41.589	53.493	0.579
144h	0.349	0.025	0.516	0.265	0.590	42.417	59.049	0.561

Table 28. Errors metrics for T_p for the month of May, where $N_v = 119$.

T_p ($N_v = 119$)								
	AME	MBE	$RMSE$	R^2	SI	$MARE$	$RRMSE$	$RMSRE$
	[m]	[m]	[m]	[-]	[-]	[%]	[%]	[-]
18h	1.479	-0.848	2.726	0.425	0.363	19.072	36.341	0.311
36h	1.305	-0.625	2.478	0.469	0.344	16.973	34.403	0.261
54h	1.721	-0.934	2.908	0.303	0.386	23.505	38.594	0.409
72h	1.529	-0.363	2.713	0.365	0.377	22.592	37.680	0.393
90h	1.853	-0.875	2.982	0.326	0.395	24.956	39.515	0.387
108h	1.759	-0.949	3.001	0.260	0.416	22.977	41.601	0.371
126h	1.897	-0.836	3.023	0.312	0.397	23.822	39.679	0.340
144h	1.500	-0.461	2.599	0.428	0.362	20.468	36.182	0.280

Table 29. Errors metrics for H_{m0} for the month of June, where $N_v = 115$.

H_{m0} ($N_v = 115$)								
	AME	MBE	$RMSE$	R^2	SI	$MARE$	$RRMSE$	$RMSRE$
	[m]	[m]	[m]	[-]	[-]	[%]	[%]	[-]
18h	0.127	0.011	0.165	0.964	0.124	13.425	12.400	0.194
36h	0.201	0.012	0.272	0.887	0.206	17.293	20.638	0.230
54h	0.220	0.067	0.302	0.875	0.223	21.484	22.347	0.346
72h	0.270	0.028	0.353	0.816	0.257	23.659	25.701	0.325
90h	0.291	0.058	0.421	0.767	0.300	26.683	30.004	0.419
108h	0.366	0.016	0.512	0.620	0.362	32.269	36.172	0.508
126h	0.416	-0.073	0.625	0.484	0.434	35.584	43.422	0.586
144h	0.531	-0.088	0.748	0.240	0.510	44.780	51.002	0.747

Table 30. Errors metrics for T_p for the month of June, where $N_v = 115$.

T_p ($N_v = 115$)								
	AME	MBE	$RMSE$	R^2	SI	$MARE$	$RRMSE$	$RMSRE$
	[m]	[m]	[m]	[-]	[-]	[%]	[%]	[-]
18h	0.819	-0.020	1.488	0.513	0.220	12.090	21.956	0.193
36h	0.808	0.107	1.391	0.530	0.212	13.160	21.216	0.212
54h	1.036	-0.017	1.637	0.416	0.243	15.807	24.276	0.228
72h	1.069	0.198	1.686	0.285	0.252	17.845	25.222	0.291
90h	1.390	-0.222	2.261	-0.237	0.332	20.649	33.170	0.320
108h	1.282	-0.020	2.052	-0.116	0.304	20.739	30.406	0.344
126h	1.561	-0.356	2.322	-0.307	0.340	24.482	34.005	0.372
144h	1.773	-0.106	2.537	-0.631	0.372	28.408	37.152	0.430

Table 31. Errors metrics for H_{m0} for the month of July, where $N_v = 77$.

H_{m0} $(N_v = 77)$								
	AME	MBE	$RMSE$	R^2	SI	$MARE$	$RRMSE$	$RMSRE$
	[m]	[m]	[m]	[-]	[-]	[%]	[%]	[-]
18h	0.164	-0.056	0.220	0.919	0.175	15.706	17.524	0.212
36h	0.199	-0.065	0.271	0.883	0.215	20.458	21.473	0.289
54h	0.188	-0.048	0.258	0.881	0.203	18.682	20.269	0.257
72h	0.217	0.017	0.314	0.814	0.270	27.836	26.971	0.492
90h	0.281	-0.018	0.412	0.678	0.347	30.937	34.715	0.464
108h	0.315	0.023	0.441	0.686	0.365	36.561	36.467	0.631
126h	0.368	0.009	0.479	0.594	0.388	38.503	38.762	0.659
144h	0.424	0.001	0.566	0.382	0.471	44.460	47.092	0.637

Table 32. Errors metrics for T_p for the month of July, where $N_v = 77$.

T_p $(N_v = 77)$								
	AME	MBE	$RMSE$	R^2	SI	$MARE$	$RRMSE$	$RMSRE$
	[m]	[m]	[m]	[-]	[-]	[%]	[%]	[-]
18h	0.782	-0.078	1.427	0.412	0.237	13.443	23.740	0.223
36h	0.791	-0.196	1.352	0.443	0.208	13.567	20.817	0.278
54h	0.742	-0.125	1.146	0.520	0.187	12.092	18.714	0.164
72h	0.945	-0.161	1.553	0.149	0.248	16.310	24.758	0.297
90h	0.962	-0.107	1.495	0.197	0.250	16.900	24.982	0.258
108h	1.258	-0.215	1.883	-0.139	0.298	20.629	29.847	0.289
126h	1.097	0.329	1.520	0.152	0.253	20.114	25.259	0.283
144h	1.051	0.128	1.435	0.286	0.228	18.849	22.834	0.306

Table 33. Errors metrics for H_{m0} for the month of August, where $N_v = 71$.

H_{m0} ($N_v = 71$)								
	AME	MBE	$RMSE$	R^2	SI	$MARE$	$RRMSE$	$RMSRE$
	[m]	[m]	[m]	[-]	[-]	[%]	[%]	[-]
18h	0.135	-0.065	0.182	0.876	0.149	11.444	14.889	0.146
36h	0.179	-0.115	0.240	0.809	0.192	14.362	19.238	0.179
54h	0.221	-0.019	0.291	0.714	0.238	20.310	23.772	0.289
72h	0.242	-0.005	0.338	0.663	0.268	19.681	26.809	0.266
90h	0.336	0.026	0.448	0.472	0.363	29.022	36.278	0.417
108h	0.322	-0.064	0.459	0.444	0.376	27.243	37.613	0.363
126h	0.405	-0.043	0.553	0.177	0.479	40.040	47.868	0.612
144h	0.483	-0.014	0.662	-0.191	0.608	58.927	60.818	1.030

Table 34. Errors metrics for T_p for the month of August, where $N_v = 71$.

T_p ($N_v = 71$)								
	AME	MBE	$RMSE$	R^2	SI	$MARE$	$RRMSE$	$RMSRE$
	[m]	[m]	[m]	[-]	[-]	[%]	[%]	[-]
18h	0.701	-0.207	1.098	0.399	0.174	10.913	17.419	0.152
36h	0.716	-0.231	1.181	0.131	0.185	10.802	18.514	0.158
54h	0.880	-0.220	1.400	0.338	0.213	13.998	21.320	0.222
72h	0.737	-0.050	1.073	0.737	0.157	11.315	15.731	0.159
90h	0.923	-0.034	1.344	0.588	0.196	15.297	19.588	0.232
108h	0.932	-0.274	1.553	0.564	0.221	12.774	22.104	0.186
126h	1.339	-0.179	2.012	0.107	0.292	20.742	29.230	0.337
144h	1.385	-0.461	2.146	0.270	0.306	22.044	30.575	0.376

Table 35. Errors metrics for H_{m0} for the month of September, where $N_v = 112$.

H_{m0} ($N_v = 112$)								
	AME	MBE	$RMSE$	R^2	SI	$MARE$	$RRMSE$	$RMSRE$
	[m]	[m]	[m]	[-]	[-]	[%]	[%]	[-]
18h	0.174	-0.038	0.229	0.936	0.159	14.393	15.904	0.183
36h	0.165	-0.070	0.216	0.937	0.151	13.994	15.052	0.186
54h	0.234	-0.102	0.327	0.885	0.215	16.692	21.498	0.218
72h	0.252	-0.032	0.332	0.888	0.210	19.211	21.049	0.272
90h	0.252	-0.030	0.382	0.870	0.231	17.496	23.088	0.245
108h	0.385	-0.058	0.552	0.713	0.325	24.988	32.471	0.350
126h	0.457	-0.143	0.659	0.581	0.384	27.429	38.405	0.388
144h	0.514	-0.168	0.770	0.445	0.427	27.874	42.741	0.375

Table 36. Errors metrics for T_p for the month of September, where $N_v = 112$.

T_p ($N_v = 112$)								
	AME	MBE	$RMSE$	R^2	SI	$MARE$	$RRMSE$	$RMSRE$
	[m]	[m]	[m]	[-]	[-]	[%]	[%]	[-]
18h	0.769	-0.059	1.268	0.640	0.175	11.293	17.479	0.199
36h	0.742	-0.144	1.536	0.535	0.209	9.976	20.928	0.189
54h	0.862	-0.123	1.471	0.514	0.202	12.185	20.206	0.224
72h	0.941	0.014	1.584	0.453	0.217	12.936	21.701	0.211
90h	0.993	-0.074	1.719	0.286	0.236	14.164	23.596	0.258
108h	1.141	-0.054	1.728	0.171	0.238	16.220	23.798	0.247
126h	1.266	0.059	1.900	0.025	0.263	18.377	26.264	0.300
144h	1.399	0.096	2.064	-0.062	0.281	21.753	28.070	0.383

Table 37. Errors metrics for H_{m0} for the month of October, where $N_v = 122$.

H_{m0} ($N_v = 122$)								
	AME	MBE	$RMSE$	R^2	SI	$MARE$	$RRMSE$	$RMSRE$
	[m]	[m]	[m]	[-]	[-]	[%]	[%]	[-]
18h	0.177	-0.070	0.254	0.950	0.131	10.684	13.090	0.149
36h	0.227	-0.061	0.307	0.926	0.158	12.798	15.823	0.165
54h	0.281	0.013	0.440	0.839	0.232	14.941	23.199	0.203
72h	0.313	-0.080	0.461	0.812	0.246	17.624	24.578	0.237
90h	0.381	-0.041	0.556	0.709	0.305	20.885	30.486	0.284
108h	0.430	-0.053	0.603	0.635	0.338	25.502	33.820	0.355
126h	0.463	-0.055	0.686	0.523	0.394	27.731	39.358	0.406
144h	0.520	-0.089	0.741	0.448	0.423	32.456	42.301	0.458

Table 38. Errors metrics for T_p for the month of October, where $N_v = 122$.

T_p ($N_v = 122$)								
	AME	MBE	$RMSE$	R^2	SI	$MARE$	$RRMSE$	$RMSRE$
	[m]	[m]	[m]	[-]	[-]	[%]	[%]	[-]
18h	0.934	-0.347	1.739	0.540	0.217	10.695	21.736	0.160
36h	0.972	0.041	1.627	0.549	0.212	12.972	21.160	0.211
54h	1.030	-0.176	1.743	0.498	0.223	12.642	22.335	0.177
72h	1.315	0.138	2.112	0.207	0.279	18.834	27.881	0.321
90h	1.452	-0.081	2.368	0.032	0.308	18.725	30.810	0.302
108h	1.302	0.028	1.961	0.295	0.262	17.944	26.229	0.266
126h	1.814	0.012	2.843	-0.176	0.367	23.731	36.660	0.374
144h	1.739	0.223	2.527	-0.136	0.342	25.574	34.248	0.392

Table 39. Errors metrics for H_{m0} for the month of November, where $N_v = 105$.

H_{m0} $(N_v = 105)$								
	AME	MBE	$RMSE$	R^2	SI	$MARE$	$RRMSE$	$RMSRE$
	[m]	[m]	[m]	[-]	[-]	[%]	[%]	[-]
18h	0.152	-0.071	0.209	0.944	0.129	10.208	12.921	0.127
36h	0.204	-0.079	0.298	0.888	0.182	13.010	18.215	0.171
54h	0.224	-0.048	0.324	0.861	0.204	15.362	20.419	0.229
72h	0.236	-0.036	0.332	0.862	0.209	15.419	20.916	0.195
90h	0.271	-0.005	0.388	0.825	0.241	18.093	24.075	0.277
108h	0.312	-0.036	0.440	0.778	0.270	19.496	27.001	0.264
126h	0.393	-0.068	0.575	0.623	0.350	26.298	35.015	0.378
144h	0.519	-0.092	0.713	0.422	0.440	32.669	43.961	0.446

Table 40. Errors metrics for T_p for the month of November, where $N_v = 105$.

T_p $(N_v = 105)$								
	AME	MBE	$RMSE$	R^2	SI	$MARE$	$RRMSE$	$RMSRE$
	[m]	[m]	[m]	[-]	[-]	[%]	[%]	[-]
18h	1.127	0.190	2.076	0.352	0.268	15.722	26.780	0.318
36h	1.273	0.229	2.419	-0.003	0.311	19.735	31.089	0.459
54h	1.361	0.042	2.401	0.259	0.305	17.846	30.516	0.337
72h	1.079	0.145	1.956	0.373	0.252	16.806	25.223	0.364
90h	1.763	0.166	3.155	-0.310	0.407	23.973	40.713	0.476
108h	1.380	0.379	2.375	0.154	0.304	20.930	30.445	0.431
126h	1.707	0.089	2.989	-0.372	0.390	23.267	38.952	0.414
144h	1.459	0.088	2.334	-0.022	0.305	19.958	30.461	0.340

Table 41. Errors metrics for H_{m0} for the month of December, where $N_v = 39$.

H_{m0} ($N_v = 39$)								
	AME	MBE	$RMSE$	R^2	SI	$MARE$	$RRMSE$	$RMSRE$
	[m]	[m]	[m]	[-]	[-]	[%]	[%]	[-]
18h	0.119	-0.020	0.154	0.975	0.084	7.556	8.417	0.096
36h	0.272	-0.026	0.378	0.854	0.203	14.970	20.329	0.198
54h	0.584	-0.334	0.807	0.374	0.428	31.720	42.797	0.439
72h	0.785	-0.420	1.137	-0.291	0.585	38.336	58.466	0.489
90h	0.766	-0.245	1.026	-0.080	0.532	40.794	53.197	0.558
108h	0.725	-0.299	1.056	-0.113	0.546	36.143	54.614	0.450
126h	0.797	-0.301	1.077	-0.227	0.561	42.320	56.052	0.531
144h	0.789	-0.358	1.029	-0.358	0.547	44.665	54.680	0.581

Table 42. Errors metrics for T_p for the month of December, where $N_v = 39$.

T_p ($N_v = 39$)								
	AME	MBE	$RMSE$	R^2	SI	$MARE$	$RRMSE$	$RMSRE$
	[m]	[m]	[m]	[-]	[-]	[%]	[%]	[-]
18h	0.987	-0.586	2.026	-0.074	0.246	9.737	24.551	0.165
36h	0.946	0.212	1.628	0.173	0.220	13.762	22.001	0.222
54h	1.306	-0.006	1.900	-0.588	0.243	17.622	24.300	0.271
72h	1.675	-0.194	2.427	-0.336	0.308	22.132	30.808	0.324
90h	1.869	-0.367	2.427	-1.315	0.296	23.721	29.615	0.329
108h	1.829	-0.327	2.663	-0.718	0.327	22.193	32.690	0.320
126h	1.752	0.022	2.375	-0.959	0.292	21.731	29.159	0.310
144h	2.271	-0.011	2.879	-2.249	0.376	31.734	37.586	0.451

The variation of the $RRMSE$ on a monthly basis is depicted in Fig. 18 and 19 for H_{m0} and T_p respectively. The $RRMSE$ is shown as a function of the forecast horizon for the twelve months and for all the data points. As mentioned previously, the gray area on the figures can be considered as the limit of accuracy for the forecast model. It is again easy to notice that the model is more accurate in predicting wave heights than wave periods. It is important to mention that the number of data points for each month varies significantly. The month of December is especially under represented and this can explain the behaviour seen in Fig. 18. The forecast model leads to overall good prediction of H_{m0} for 2.5 to up to 5 days ahead.

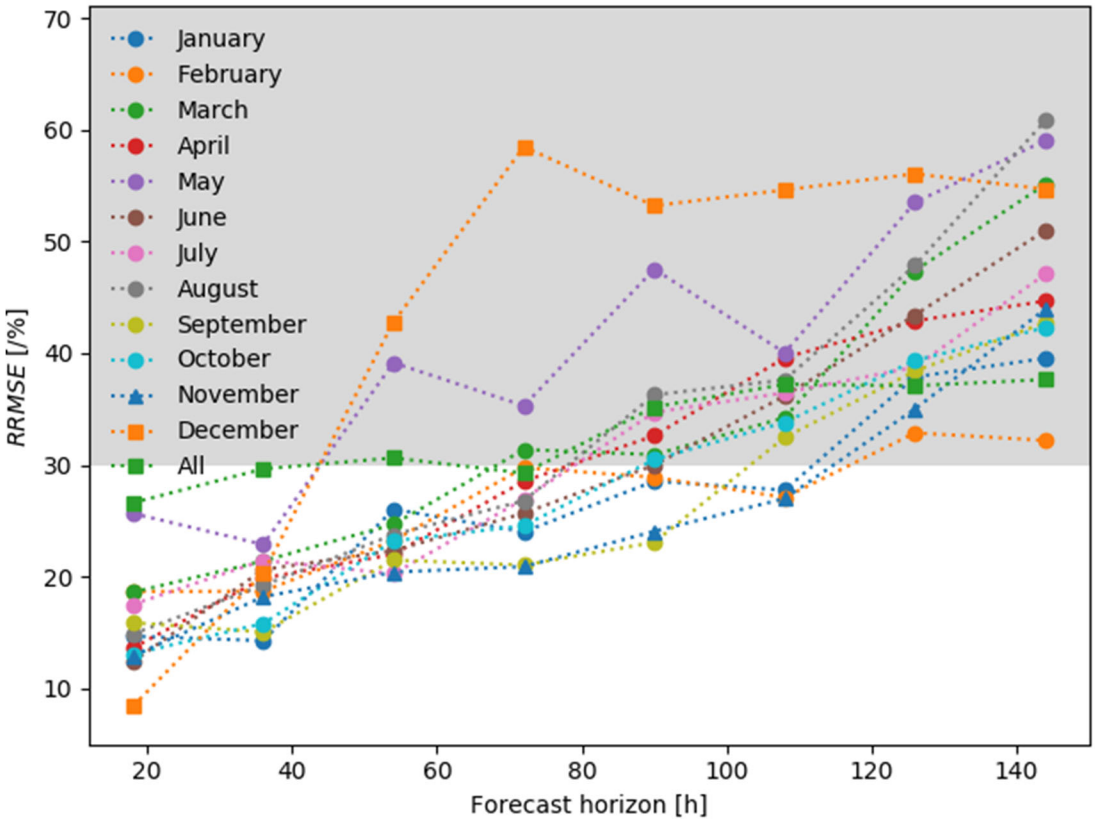

Fig. 18. *RRMSE* of H_{m0} as a function of the forecast horizon for the twelve months of the year. The *RRMSE* as a function of the forecast horizon for the whole period is also shown. The grey area can be considered as the limit of accuracy for the forecast model.

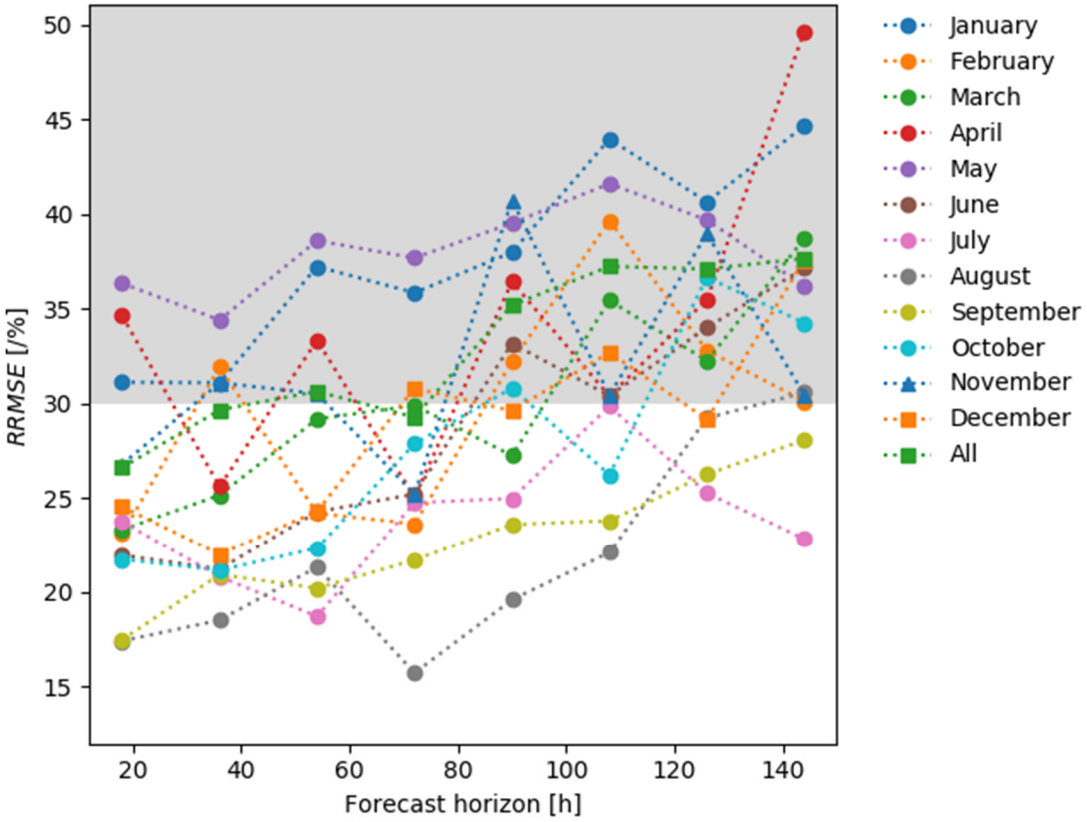

Fig. 19. *RRMSE* of T_p as a function of the forecast horizon for the twelve months of the year. The *RRMSE* as a function of the forecast horizon for the whole period is also shown. The grey area can be considered as the limit of accuracy for the forecast model.

Conclusion

In this work, the forecast model for the DanWEC test center was introduced. The model is strongly based on a hindcast model for the area, which has been validated using measured data from wave measuring buoys placed at the test center. The forecast model provides a 5½ days-horizon for a range of parameters enabling a better planning of O&M activities at the test center. An evaluation of the accuracy of the prediction given by the forecast model was performed. Several errors metrics were calculated and presented on a seasonal and monthly basis. Results have shown that the model is better at predicting wave heights than wave periods, and is mostly under predicting both H_{m0} and T_p. The model can be considered giving good prediction for a horizon of 2.5 days throughout the year and up to 5 days for some of the autumn and summer months.

Future work includes data assimilation from the wave measuring buoys into the forecast model in order to increase the accuracy of the prediction and thereby a better planning of the O&M at the test center.

References

[1] Brodersen, H. J., Nielsen, K., Kofoed, J.P.: Development of the Danish test site DanWEC. In: 10th European Wave and Tidal Energy Conference (EWTEC), Aalborg, Denmark (2013)

[2] DHI: MIKE 21, Spectral Wave Module, Scientific Documentation. DHI Hørsholm, Denmark (2015)

[3] Tetu, A., Kofoed, J.P.: Long-term wave climate at DanWEC. DCE Contract Report No. 188, Department of Civil Engineering, Aalborg Univeristy (2017)

[4] Rugbjerg, M., Sørensen, O. R., Jacobsen, V.: Wave Forecasting For Offshore Wind Farms. In: 9th International Workshop on Wave Hindcasting and Forecasting, Victoria, B.C., Canada (2006)

[5] Nielsen, K., Remmer, M.,Beatie, W.C.: Elements of large wave power plants. In: 1st European Wave and Tidal Energy Conference (EWTEC). NEL-Renewable Energy, Edinburgh, UK (1993)

[6] Datawell BV 2014: Datawell Waves4 Manual, User Manual. Datawell BV oceanographic instruments (2014)

[7] MIKE 21 SW, https://www.mikepoweredbydhi.com/products/mike-21/waves

[8] Jensen, R. E., Cardone, V. J., Cox, A.T.: Performance of third generation wave models in extreme hurricanes. In: 9th International Wind and Wave Workshop, Victoria, B.C., Canada (2006)

[9] Battjes, J., Stive, M.: Calibration and verification of a dispersion model for random breaking waves. Geophys. Research., Vol. 112, pp. 307-319 (1985)

[10] Kaminsky, G.: Evaluation of depth-limited wave breaking criteria. In: 2nd International Symposium on Ocean Wave Measurement and Analysis, New Orleans, USA (1993)

[11] Jensen, P. M.: DanWEC EUDP, Establishment ofWave Hindcast. Technical report, DHI (2016)

[12] M.-F Li, X.-P. Tang, W. Wu and H.B. Liu : General models for estimating daily global solar radiation for different solar radiation zones in mainland China. Energy Conversion and Management, Vol. 70, pp. 139-148 (2013).